Universitatea POLITEHNICA din Bucureşti
Facultatea de Electronică, Telecomunicaţii şi Tehnologia Informaţiei

Sistem auto de climatizare eficientă pe patru zone de temperatură - HVAC

Lucrare de dizertaţie

Prezentată ca cerinţă parţială pentru obţinerea titlului de
Master în domeniul *Electronică şi Telecomunicaţii*

programul de studii de masterat
Tehnologii avansate integrate în ingineria electronicii auto (TAEA)

Conducător ştiinţific
Conf. Univ. Dr. Ing. Alexandru VASILE

Absolvent
ing. Adrian-Ioan LIŢĂ

2014

Declaraţie de onestitate academică

Prin prezenta declar că lucrarea cu titlul "Sistem auto de climatizare eficientă pe patru zone de temperatură - HVAC", prezentată în cadrul Facultăţii de Electronică, Telecomunicaţii şi Tehnologia Informaţiei a Universităţii POLITEHNICA din Bucureşti ca cerinţă parţială pentru obţinerea titlului de *Master* în domeniul *Electronică şi Telecomunicaţii*, programul de studii *Tehnologii avansate integrate în ingineria electronicii auto (TAEA)* este scrisă de mine şi nu a mai fost prezentată niciodată la o facultate sau instituţie de învăţământ superior din ţară sau străinătate.

Declar că toate sursele utilizate, inclusiv cele de pe Internet, sunt indicate în lucrare, ca referinţe bibliografice. Fragmentele de text din alte surse, reproduse exact, chiar şi în traducere proprie din altă limbă, sunt scrise între ghilimele şi fac referinţă la sursă. Reformularea în cuvinte proprii a textelor scrise de către alţi autori face referinţă la sursă. Înţeleg că plagiatul constituie infracţiune şi se sancţionează conform legilor în vigoare.

Declar că toate rezultatele simulărilor, experimentelor şi măsurătorilor pe care le prezint ca fiind făcute de mine, precum şi metodele prin care au fost obţinute, sunt reale şi provin din respectivele simulări, experimente şi măsurători. Înţeleg că falsificarea datelor şi rezultatelor constituie fraudă şi se sancţionează conform regulamentelor în vigoare.

Bucureşti, *Iulie 2014*
Adrian-Ioan LIŢĂ

_____
(semnătura în original)

POLITEHNICA University of Bucharest
Faculty of Electronics, Telecommunications and Information Technology

Four temperature zones efficient climate control automotive system - HVAC

Dissertation Thesis

Submitted in partial fulfillment of the requirements for the degree of
Master of Science in the domain *Electronics and Telecommunications*

Master study program
Advanced Integrated Technologies in Automotive Engineering

Thesis advisor
Conf. Univ. Dr. Ing. Alexandru VASILE

Student
Ing. Adrian-Ioan LIŢĂ

2014

Statement of academic honesty

I hereby declare that the thesis “Four temperature zones efficient climate control automotive system - HVAC”, submitted to the Faculty of Electronics, Telecommunications and Information Technology in partial fulfillment of the requirements for the degree of *Master of Science* in the domain *Electronics and Telecommunications*, study program *Advanced Integrated Technologies in Automotive Engineering*, is written by myself and was never before submitted to any other faculty or higher learning institution in Romania or any other country.

I declare that all information sources I used, including the ones I found on the Internet, are properly cited in the thesis as bibliographical references. Text fragments cited “as is” or translated from other languages are written between quotes and are referenced to the source. Reformulation using different words of a certain text is also properly referenced. I understand plagiarism constitutes an offence punishable by law.

I declare that all the results I present as coming from simulations and measurements I performed, together with the procedures used to obtain them, are real and indeed come from the respective simulations and measurements. I understand that data faking is an offence punishable according to the University regulations.

Bucharest, *July 2014*
Adrian-Ioan LIȚĂ

_____
(Student’s signature)

Table of Contents

Table of Figures

Table of Tables

Table of Acronyms and Abbreviations

ADC = analog to digital converter
ASIC = application specific integrated circuit
BLDC = brushless DC motor
BOM = bill of materials
CAN = controller area network
DC = direct current
FOC = field oriented control
HVAC = heating, ventilation and air conditioning
I^2C= inter-integrate circuit (communication bus)
IPM = interior permanent magnet
LIN = local interconnect network
MOS-FET = metal oxide semiconductor – field effect transistor
NRZ = non-return to zero
NTC = negative temperature coefficient
(E)OBD – (enhanced) on-board diagnostics
PMSM = permanent magnet synchronous motor
PTC = positive temperature coefficient
QEI = quadrature encoder interface
SMPS = switched mode power supply
SPI = serial peripheral interface
SPM = surface permanent magnet
SUV = sport utility vehicle
SVM = space-vector modulation
UART = universal asynchronous receive transmit
UNI/O = asynchronous serial bus which uses one wire
(E)USART = (enhanced) universal synchronous asynchronous receive transmit

Chapter I. HVAC systems introduction

Air conditioning was first introduced as optional package in 1933 (1), manufactured and installed by a 3rd party American firm who sold it for a 2007 equivalent of $4000. Later, in 1940 and 1941 other manufacturers started doing so (2). The first car to have a complete heating, ventilation and air conditioning system installed was the American automobile Nash Ambassador (2).

Modern HVAC systems use the engine's power to refrigerate the air. The switching on and off of the evaporator is done with a coil which couples or decouples compressor's shaft from the main driving belt. Depending on the control system present on the car, switching on and off the air conditioning can be done either manually (in classical air conditioning systems) or automatically (in automatic climate control systems).

Classic air conditioning (low-end) systems have only one climate zone – the whole interior volume. Most systems nowadays offer two zone of climate control, one for the left and one for the right side of the interior. High-end systems offer four zone climate allowing each passenger to set the desired temperature and climate.

The following paragraphs will briefly present a four zone climate control system, in terms of mechanics, fluid mechanics and thermodynamics (3).

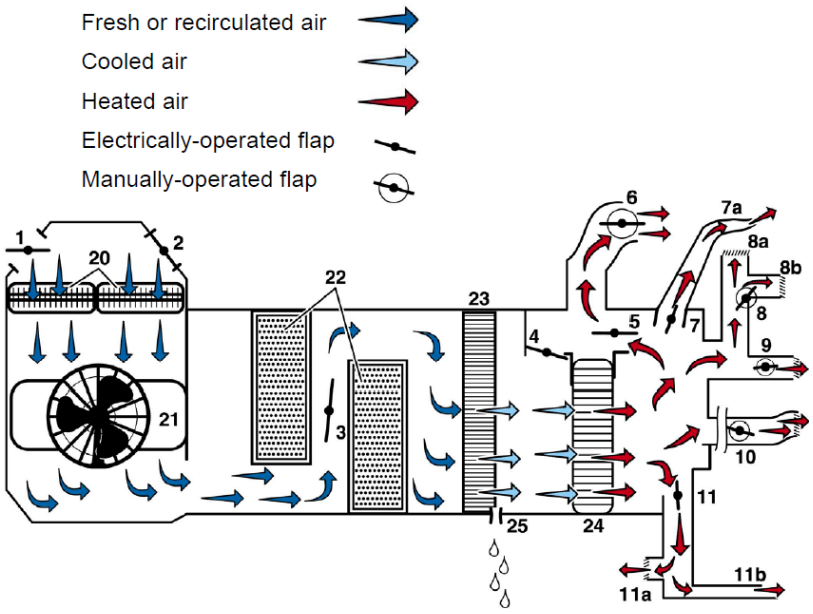

1 - Fresh air flap
2 - Recirculated air flap
3 - Activated charcoal flap
4 - Center outlet diverter flap
5 - Center outlet blend flap
6 - Center outlet
7 - Defroster outlet
8 - Side outlet flap
9 - Rear side compartment flap
10 - Rear compartment flap
11 - Footwell flap
20 - Dust filters
21 - Blower motor
22 - Activated charcoal filter
23 - Evaporator
24 - Heat exchanger

Figure I.1 Airflow - Heating mode (3)

The schematic in *Figure I.1* presents the airflow in the dashboard of a HVAC system. This is where the air is filtered and the temperature is adjusted. Afterwards it is pushed through one or more of the trap doors (4, 5, 7 and 11). Trap doors 1 and 2 control the input air from the car. Switching them can input the air either from outside (fresh) or from inside (recirculated).

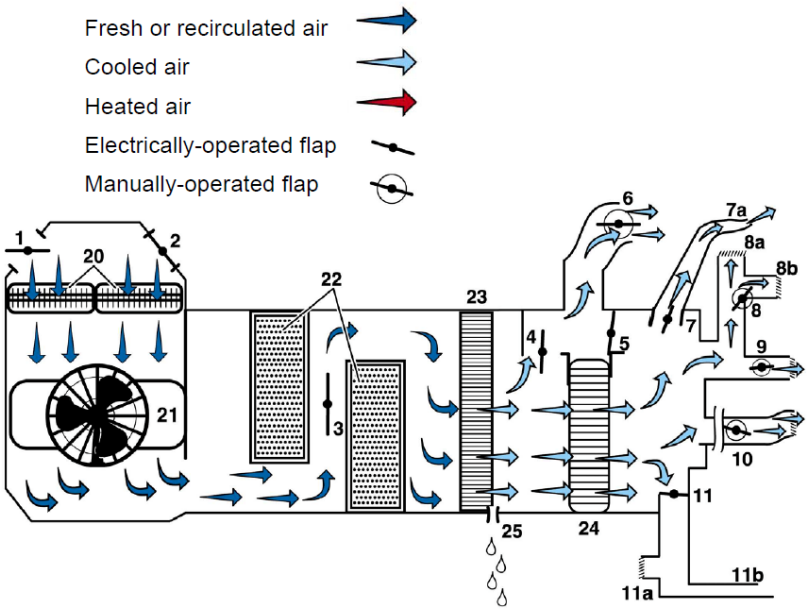

1 - Fresh air flap
2 - Recirculated air flap
3 - Activated charcoal flap
4 - Center outlet diverter flap
5 - Center outlet blend flap
6 - Center outlet
7 - Defroster outlet
8 - Side outlet flap
9 - Rear side compartment flap
10 - Rear compartment flap
11 - Footwell flap
20 - Dust filters
21 - Blower motor
22 – Activated charcoal filter
23 - Evaporator
24 - Heat exchanger

Figure I.2 Airflow - Cooling mode (3)

Figure I.1 and *Figure I.2* are practically the same system, one for heating and one for cooling. The difference between them is that the position of the trap doors (flaps) is set to either cooling or heating, and the heat exchanger is turned on, respectively off.

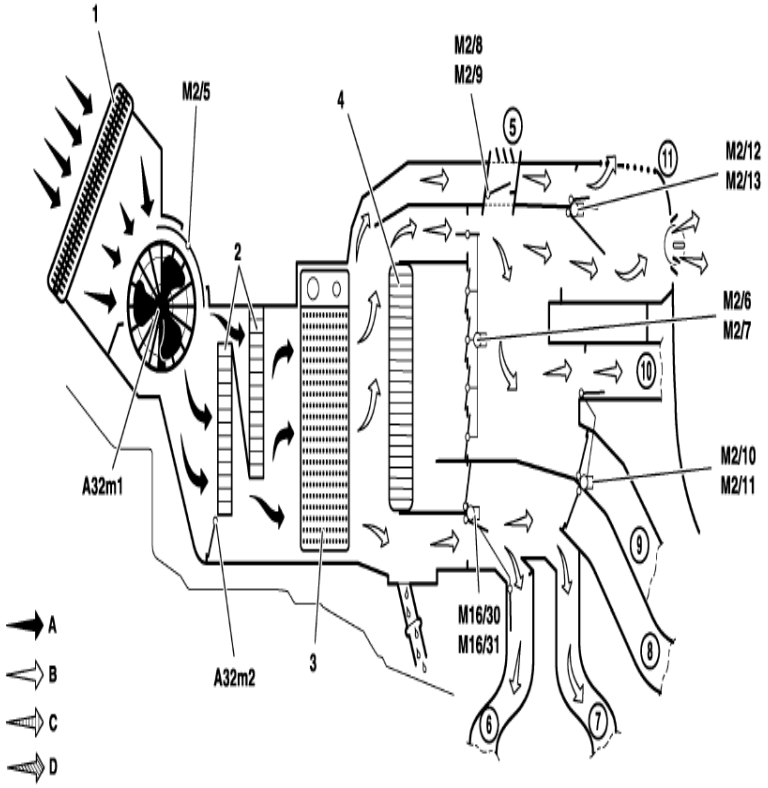

A - Fresh / recirculated air
B- Cooled air
C - Heated air
D - Blend air
3 - Evaporator
4 - Heat exchanger
5 - Defroster outlet
6 - Center outlet
7 - Rear footwell
8 - Left front footwell
9 - Right front footwell
10 - Front lateral outlet
11 - Front center outlet
A32m1 - Blower motor
M2/5 - Fresh/recirculate actuator
M2/6 - Left blend flap actuator
M2/7 - Right blend flap actuator
M2/8 - Left defroster actuator
M2/9 - Right defroster actuator
M2/10 -Left footwell actuator
M2/11 - Right footwell actuator
M2/12 - Left center actuator
M2/13 - Right center actuator
M16/30 Left rear actuator
M16/31 - Right rear actuator

Figure I.3 4 Zone Climate Control System (4)

Figure I.3 represents a four-zone climate control system schematic. At a brief analysis one blower motor and 11 flaps are present in the schematic, which mean at least 11 stepper motors. Also, on top of that the AC compressor can also be considered as being an electric motor – recently, high-tech HVAC systems use electric compressor instead of a belt-driven

one because, first of all it proved to have higher efficiency, and second, some small cars (such as Smart) have small engines and a hydraulic compressor is harder to switch on and off, which reduces power and torque.

Figure I.4 Audi Q7 4 Zone Climate Control System (5)

Figure I.4 is a perfect example of the four zone climate control system, this one being installed into Audi Q7 SUV. This particular example uses two blower motors because the interior volume is considerably greater, and having four zones to control requires air pushed through many doors. This is just to give a general idea of the principle involved in four-zone climate control systems.

Chapter II. Overview of the electrical system

The electrical system resides on efficiently controlling the blower motor *Figure I.2* (21), the flaps motors (1, 2, 4, 5, etc.).

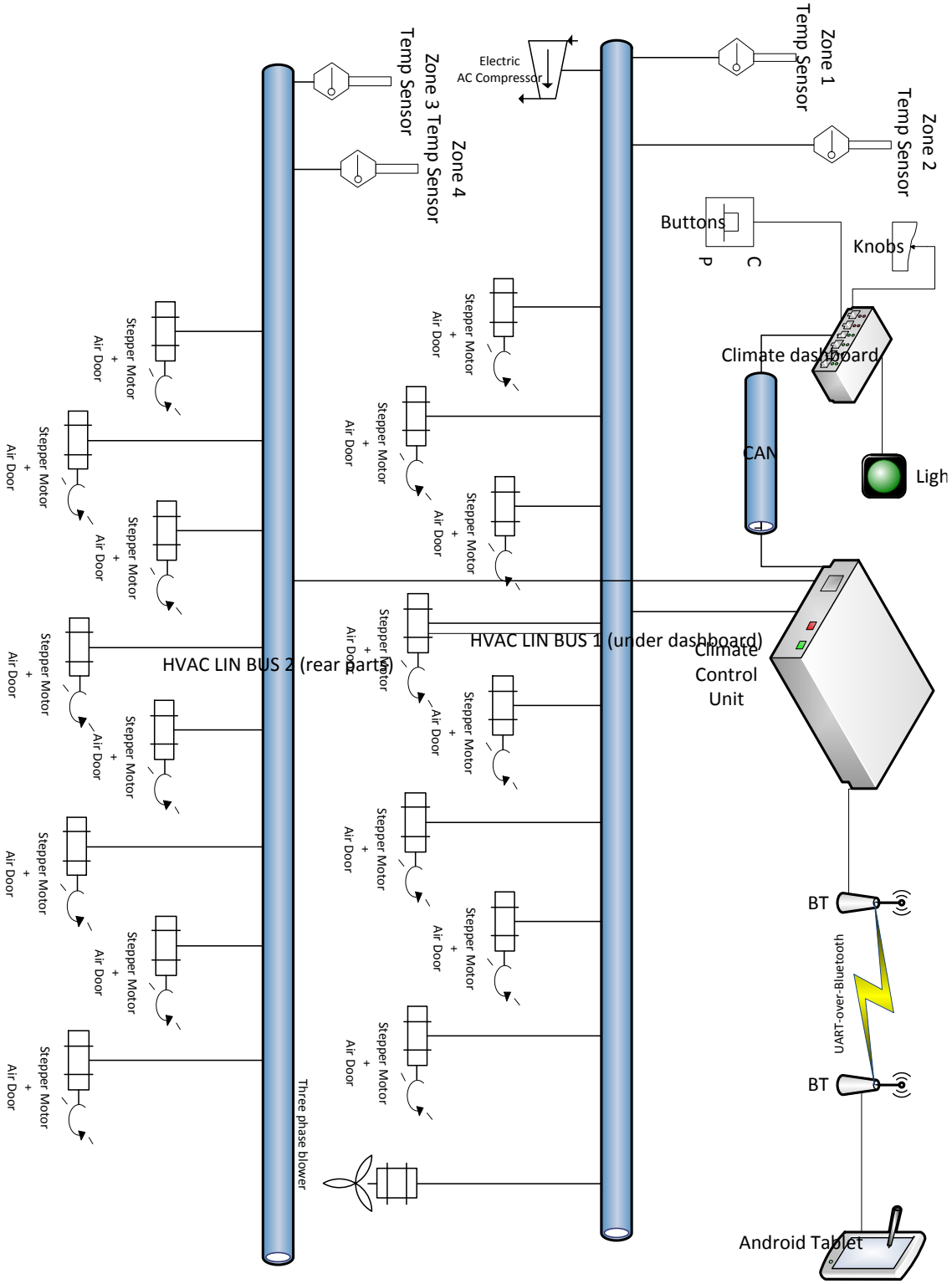

Figure II.1 Overview of the electrical system built in the present thesis

Subchapter 1 Premises

The main premises of this project are as follows:

- Maximum efficiency, making the whole system as “green” as possible;
- Minimum cost is considered without compromising efficiency, security or integrity;
- As the project is built in collaboration with Microchip Technology Inc., most of the parts used are from Microchip’s portfolio;
- Having one part of each subsystems built, with the main system and buses supporting all the necessary parts for a full four-zone climate control system.

Subchapter 2 Communication

This project uses LIN and CAN protocols for automotive communication; for debugging reasons Bluetooth is also used to wirelessly communicate and send debugging data. Since Bluetooth is not part of an automotive HVAC system, Bluetooth will not be treated by this paper.

The main difference between LIN and CAN consists of price (CAN being more expensive in terms of licensing (6)) and operating mode. Usually CAN provides interconnectivity over the whole car, connecting the more important parts (such as engine communication, dashboard, lightning system, etc.) with various optional systems, such as the climate system. Communicating within one system LIN protocol is used because of the following reasons:

- may require a lot of devices on the bus (for example, the four zone climate system requires at least 12 steppers, 1 blower, 4-5 sensors, which would add up to 20 devices on the CAN bus);
- having more devices on the CAN bus will keep the bus busier
- there is no need for an auxiliary system to be able to directly communicate with an internal component (i.e.: the dashboard should not communicate to any of the stepper motors directly, but only to the climate computer, which will do the communication to the stepper motors);
- any CAN-enabled device have extra cost, just by licensing matters.

LIN protocol (6)

LIN (Local Interconnect Network) was developed at the end of the 1990s by the LIN Consortium, which was founded by BMW, Volkswagen-Audi Group, Mercedes-Benz and Volvo. The technology wasn’t new, but a spin-off provided by Volcano Automotive Group – Mentor Graphics and Motorola.

The main reason for developing LIN was that CAN was getting too expensive to implement on every device in a car and automotive manufacturers started developed proprietary buses, which led to compatibility issues. LIN version 1.3, first public release, was published in November 2002. One year after, in September 2003 LIN version 2.0 was released, adding new capabilities. By now, LIN 2.0 is the standard LIN protocol used.

Since LIN is a serial protocol over one wire, the implementation in a microcontroller is based on the UART/USART/EUSART module available, configured as eight data bits, one start and one stop bit, with no parity. LIN protocol is usually implemented with a microcontroller on the host (ex: climate computer) and with ASIC on the slaves, but since the price of LIN-capable microcontrollers tend to get lower, this may not be always true. LIN usually operates directly in 12V for higher noise rejection, and in order to achieve that a special transceiver (LIN transceiver) is used.

The LIN protocol is a master-slave type of protocol (1 master and up to 15 slaves). The LIN frame has two parts: header and response. While the response can be sent by either the master or any of the addressed slaves, the header is always sent by the master. LIN supports bit rates up to 19.2 kbit/s on a single wire which can be up to 40 meters long.

LIN supports two states: sleep and awake. Usually, to save energy, each device goes into sleep mode based on a predefined timeout value or on a predefined behavior (e.g.: a slave receives a command, executes it and goes to sleep; any other slaves go directly to sleep if they're not addressed). Upon the receiving of the WAKEUP frame, all the nodes on the bus wake up and get ready to receive the next frame from the LIN-Master.

There are 5 types of frames defined in LIN 2.0 specifications:

- unconditional frame (identifiers 0x00 to 0x3B), which is received by all the slaves;
- event-triggered frame, in which the master interrogates the slaves if any change is available;
- sporadic frame, sent by the master so a collision won't occur;
- diagnostic frame;
- user-defined frames (identifier is 0x3E)

As descried before, a frame consists of a header (always sent by the master) and a response. While the response is simple, containing only DATA (one up to eight bytes) and CHECKSUM (in order to detect errors of DATA), the header consists of five parts:

- BREAK, used to activate the slaves to listen to the other parts of the header;
- SYNC, also called synchronization byte, where the 0x55 byte is sent (which is binary 01010101) in order to synchronize the operating baud rate;
- INTER BYTE SPACE, also called synchronization break, used to adjust the bus jitter;
- IDENTIFIER, used to identify the command on a specific LIN-Slave;
- RESPONSE SPACE, time between IDENTIFIER and DATA (from the response).

In the presented application Microchip's LIN serial analyzer (*Figure II.2*) was used to debug the LIN interface. The analyzer requires three connections: Vbat (12V), LINBus and GND, plus one USB connection to a computer in order to analyze the data.

Figure II.2 Microchip LIN Serial Analyzer

CAN bus (7)

The CAN protocol was developed starting in 1983 by Bosch, and released in 1986 at the annual SAE (Society of Automotive Engineers) congress. The first CAN-enabled controller was developed by Intel and Philips, being available on the market in early 1987. Though its original development was for automotive, other industries such as aerospace, maritime and medical now use CAN for its well proven performance and reliability.

The CAN bus is the most frequently used bus standard in automotive. The bus was designed to work without a host, so every node on the bus can communicate with others, but not simultaneously. CAN works on messages, which consist of an identifier (ID) and up to 8 – on older version of CAN – or 64 – on newer version, CAN FD – bytes of data, coded NRZ and transmitted serially on the bus.

Transmission starts when any of the nodes detect the bus as being idle (5V TTL). If two nodes begin the transmission at the same time, the node with the most dominant ID (which is less in value) will pull down the line (bringing it to 0) while the less dominant ID leaves the line to 5V. When the less dominant node checks the bus and sees that for a 1 transmitted, the line replies a 0, it automatically assumes that a transmission of higher priority is in place, and reschedules the packet. This mechanism is referred to as “priority based bus arbitration” – the lower the ID, the higher the priority.

Within the CAN protocol, the ID of a message must be unique in order to avoid collision when two nodes try to send data at the same time. The best way to allocate ID is by the priority of the message. In current application, since using CAN to communicate between the climate dashboard panel and the climate computer, there is no need for immediate delivery of the message, which implies a high-value ID.

CAN bus connectors typically use 4 signals: CAN V+ and GND for power, CAN-High (CAN+) and CAN-Low (CAN-) for data transmission. Since there is no clock sent during transmission, and each node has its own clock, synchronization is achieved by dividing each bit of the frame into a number of segments: synchronization, propagation, phase 1 and phase 2. The sampling point for reading CAN data is between phase 1 and phase 2, as shown in *Figure II.3*.

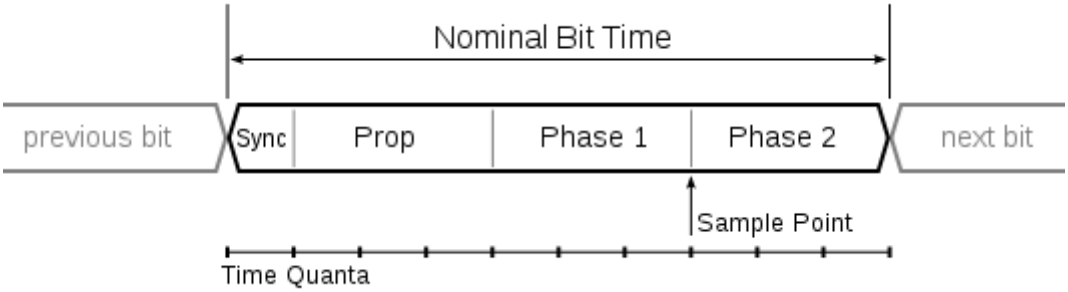

Figure II.3 CAN bit timing (7)

Since version 2.0B, CAN supports two types of framing: standard (both in CAN2.0A and CAN2.0B) and extended (only CAN2.0B), with the difference that for standard framing, the ID is 11-bit length, and for extended it is 29-bit length. To differentiate the two, the standard framing sends the IDE (ID Extender) bit as dominant, while the extended framing leaves it recessive. CAN-enabled devices that support extended frame format messages are also able to send and receive messages in CAN standard frame format.

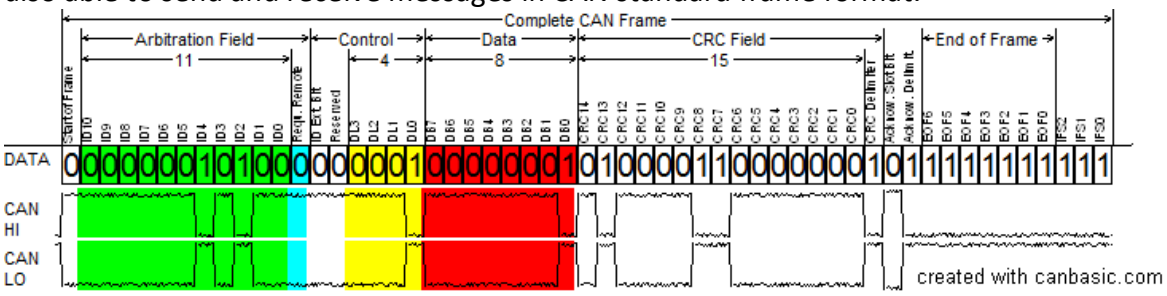

Figure II.4 CAN-Frame in base format with electrical levels without stuffbits (7)

The frame starts with the start-of-frame bit. Afterwards, on the green-highlighted part, the message identifier is sent in order for the bus to arbitrate the signal. For the control signals, the first one is the RTR (remote transmission request), which is dominant if the node is sending data, and recessive if the node is requesting data. The second control bit is the IDE (ID extender) bit, which is dominant for 11-bit length frame and recessive for 29-bit frames. After the IDE bit, there is one reserved bit left, following the data length (DL) bits (4 – yellow highlighted), which indicate how many data bytes are present in the frame. After this, the data (red) is sent, together with CRC, and acknowledge bits following it. The end of frame is marked by 7 recessive bits. However, the complete frame also requires at least 3 inter-frame recessive bits. An example of a CAN frame is presented in *Figure II.4*.

In the presented application Microchip's CAN BUS serial analyzer (*Figure II.5*) was used to debug the CAN communication. The analyzer is connected via USB to a computer in order to debug the data.

Figure II.5 Microchip CAN BUS Analyzer

Subchapter 3 Sensors

This paper treats only temperature sensors. In different climate systems other types of sensors may appear: pressure sensors and humidity sensors. Also, in the next chapters the sensorless approach for both blower motor and trap door motors is used. Otherwise, in a sensored approach the sensors for these two applications would have been incremental rotary sensors (encoders).

Considering an output based classification, temperature sensors can be either analog or digital.

Analog temperature sensors are in general based on resistors or diodes, the first being dominant. In thermal measurements there are two types of thermistors (thermal resistors): NTC and PTC thermistors. NTC thermistors' resistance value lowers with temperature, is maximum at a low temperature, and minimum at a high temperature. The PTC thermistor resistance value rises with temperature, is minimal at a minimum temperature value.

Digital sensors are in fact analog sensors put together with an ADC converter and a digital communication interface (usual interfaces for temperature are I^2C, SPI and UNI/O). For calibration and outputting, the digital communication interface contains a very limited microprocessor and few bytes of memory. Factory calibration of digital sensors implies that the manufacturer writes a small table in the sensor memory, making it easy for the microprocessor to output a value from the table based on the input of the ADC converter.

Chapter III. Blower

Until recently most blowers in automotive ventilation used brushed DC motors. This was happening due to the simplicity in usage and the low cost compared to a three-phase motor, which requires extra circuitry for command and control (since the car's voltage link is roughly 12V DC, and a three-phase motors requires three-phase AC voltage).

While writing this thesis the industry tends to go towards three-phase BLDC or PMSM motors instead of brushed DC motors for the blower, because these motors have a few advantages:

- Less acoustical noise;
- Virtually no electrical noise (no sparks);
- Longer lifetime (no brushes);
- Higher efficiency vs. DC motors.

The main disadvantage of the three-phase motor vs. the DC motor represents the control-board cost, which keeps lowering due to development of new technologies. The cost is the main factor when considering why the DC brushed motor was used for such a long time. The first ventilation systems that used a three-phase blower were the ones on high-end, executive cars, on which acoustical noise was a problem. Second such ventilation systems were also implemented on electric cars due to its efficiency and very low electric noise.

A classical three-phase motor can have sensor circuitry mounted (Hall-effect based sensors which provide an accuracy of 30 electrical degrees, or an encoder, which is usually more precise, going up to 10-15 bits of accuracy per mechanical revolution). Sensors basically provides the rotor position, in order for the electrical circuit to know how much voltage/current to apply to each of the three phases. The main disadvantages when using sensors are that they add cost to the system and they can get damaged, while the main advantage is that the calculations are very low when using sensored techniques of motor control, which lowers the microcontroller's price.

There are two methods for controlling three-phase motor: trapezoidal control and sinusoidal control (i.e.: scalar control and vector control).

Trapezoidal control applies voltage to two out of three phases of the motor, while leaving one unconnected. This will result in a six-step commutation algorithm. The main advantages of the trapezoidal control is that the algorithm is much easier and cost effective than it is for sinusoidal control, but the main drawbacks of the trapezoidal control is first that the current drawn by the motor will have a trapezoidal form, with lot of harmonics, and second, the position of the rotor is known every 60 electrical degrees, which means that if the load on the motor's shaft is changing faster than this, the motor may stall and fail.

Sinusoidal control assumes the current drawn by the motor (from the DC voltage) will look sinusoidal. Some advantages include having a better knowledge of the rotor's position (up to less than 1 electrical degree) and the algorithm can be designed to remove all harmonics, leaving just the fundamental. Sinusoidal control can be done in various ways, one of the most efficient in terms of torque outputted by the motor is called FOC – field oriented control – which is described in the next chapter. Also the control mechanism used in this paper is sensorless. The sensorless approach has some advantages against a sensored approach due to concerns of costs and effectiveness. The sensorless approach here used is the single-shunt current reconstruction method.

Subchapter 1 PMSM control: single-shunt sensorless FOC (8) (9)

Sensorless control of a PMSM motor refers to controlling a PMSM motor without having any sensors (either Hall sensors or QEI-based rotary encoder). Instead, a single shunt is used to measure the current through the motor, apply calculations to it and estimate the rotor's angle based on this.

Field oriented control, or vector control (10), is a motor control technique generally used in high-performance motor applications, which can operate smoothly and efficient over the whole speed range and is capable of fast acceleration and deceleration, while reducing power consumption. Size and cost are also minimized since the beginning of the digital signal microcontroller era because a practical motor control microcontroller is capable of measuring shunt signals and phase voltages, make calculations based on the measured signals and then output PWM signals to gate drivers and MOS-FET transistors in order to control the motor itself (11).

The whole vector control process can be described as follows:

1. Phase currents Ia, Ib and Ic are measured;
2. The three phase currents are then converted into a two-axis system: $I\alpha$ and $I\beta$, which are time-varying quadrature current values, as viewed from the perspective of the stator (Clarke transform);
3. The new two-axis system is the rotated to align to to the rotor flux. The two new variables are Id and Iq, which are quadrature currents transformed to the rotating coordinate system, and for a steady state, they're constant (Park transform);
4. The error signals formed from Id, Iq and reference values for each of them are feed into two PI control loops. The output of the PI loops is represented by Vd and Vq;
5. Next, a new transformation angle is estimated by the inverse Park transform, by using Id, Iq, Vd and Vq as inputs. The output is then rotated back to the stationary reference frame using the new calculated angle. This provides an output of: $V\alpha$ and $V\beta$;
6. $V\alpha$ and $V\beta$ are provided to the SVM block, which will generate the PWM patterns in order to obtain a sinusoidal current through the motor.

The whole process can be easily seen in *Figure III.1*.

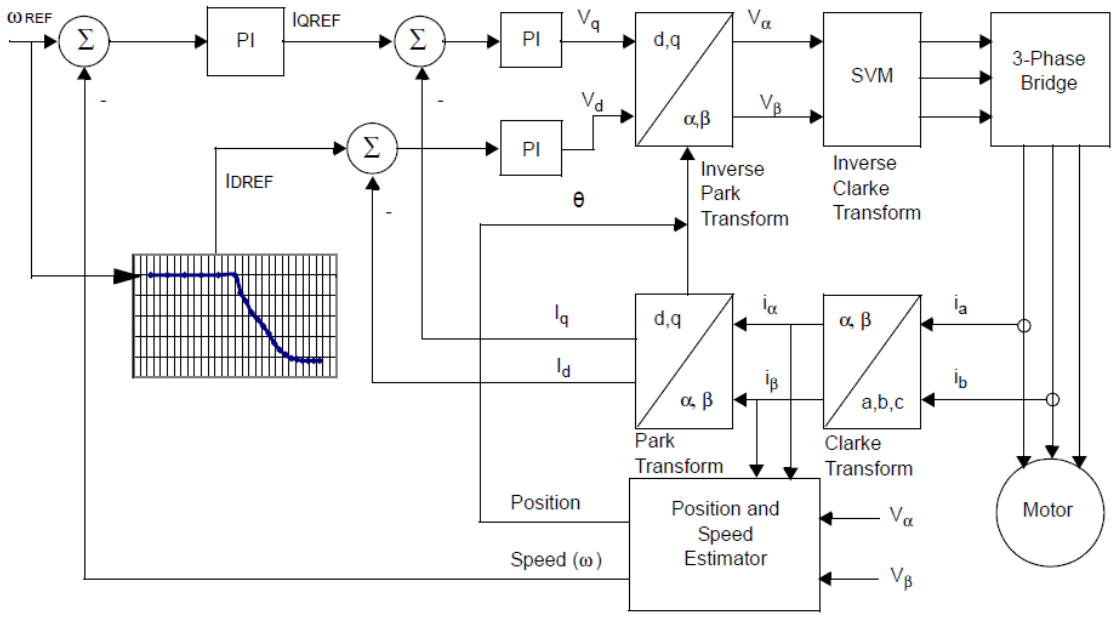

Figure III.1 FOC diagram

In order to understand the various aspects of vector control, an analysis of all current measurement techniques needs to be done: measuring all three phases (three shunts), measuring two out of three phases (dual shunt) and measuring the bus current (single-shunt).

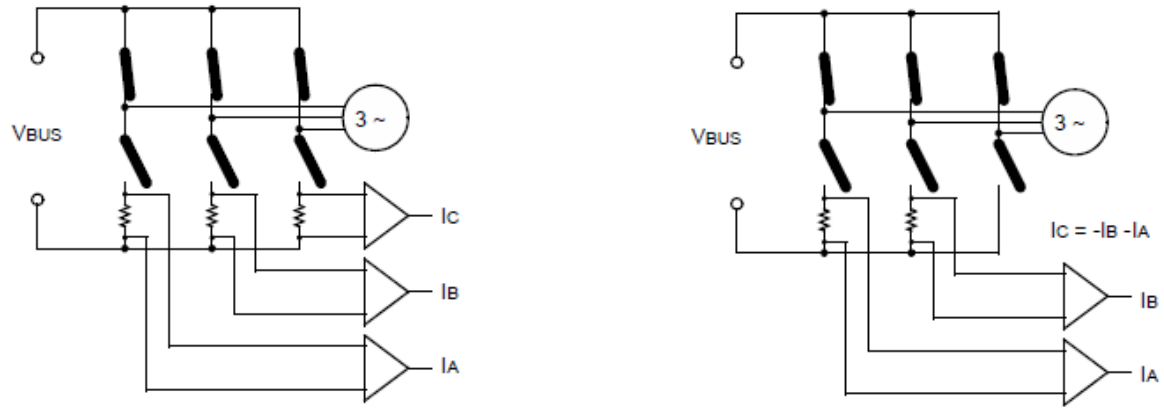

Figure III.2 Three-phase current measurement vs. dual shunt current measurement

Considering a balanced load (balanced motor: all lines have the same impedance) and applying Kirchhoff's law on the circuit in *Figure III.2*, the following is true: $Ia + Ib + Ic = 0$, which simply concludes that using three-phase current measurement system would just be redundant, since one of them (Ic for example) can be easily calculate from the other two: $Ic = -Ia - Ib$.

When using a single shunt to measure the current, neither of the phases can be measured in order to have a working system, since there will be two unknowns at all times. Instead, the current measurement here is done on the DC bus. *Figure III.3* and *Table III.1* describe both the circuitry used to measure the current and the truth table in order to measure the current on a certain phase. One advantage of the single-shunt three-phase reconstruction is cost reduction, because only one shunt is used instead of two. Second, since only one shunt resistor is used, only one operational amplifier is needed. The main

advantage here is that by not using more than one op-amp is that the gain and offset is the same for all measurements.

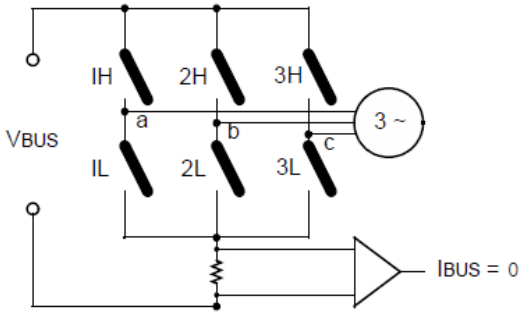

Figure III.3 Single-shunt current measurement circuitry

1H	1	0	0	0	1	1
2H	0	1	0	1	0	1
3H	0	0	1	1	1	0
1L	0	1	1	1	0	0
2L	1	0	1	0	1	0
3L	1	1	0	0	0	1
Ibus	*Ia*	*Ib*	*Ic*	*-Ia*	*-Ib*	*-Ic*

Table III.1 Single-shunt current measurement truth table

To implement sinusoidal waveform with PWM control one can choose between two modulation methods: classic sinusoidal modulation and space vector modulation (SVM) (12). The advantage of SVM over the classic approach is that while classic sinusoidal modulation can only achieve 86% of the input voltage, SVM gets to 100%.

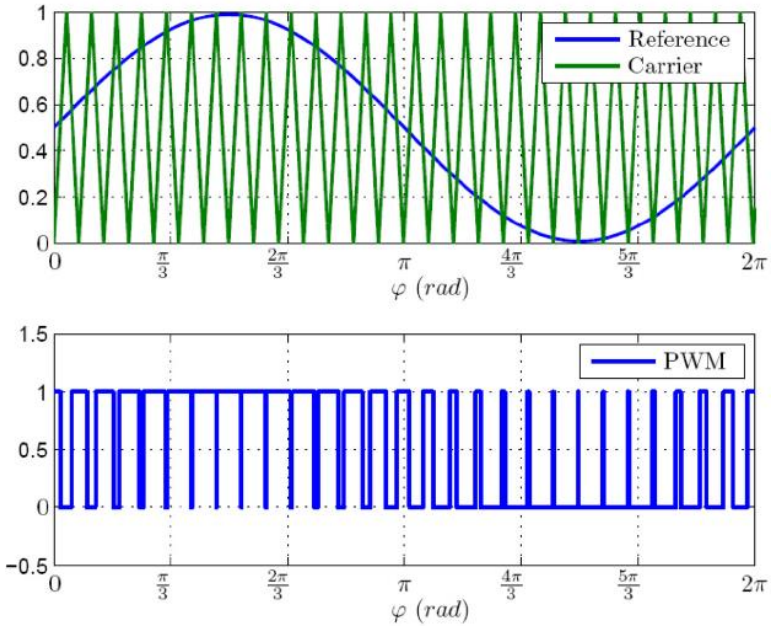

Figure III.4 Sinusoidal modulation

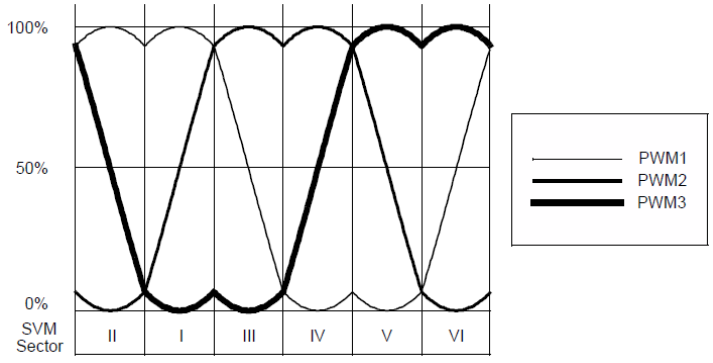

Figure III.5 Space Vector Modulation

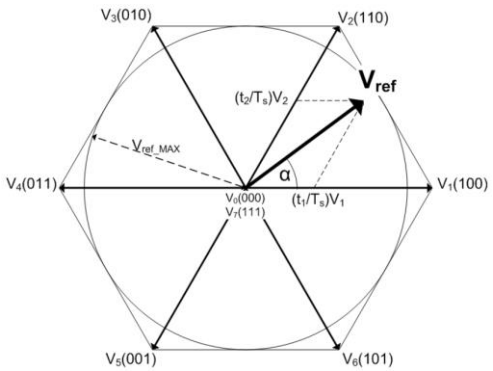

Figure III.6 SVM switching vectors

For SVM, calculating line-to-line voltage on the three phases in *Figure III.5* will result a sinusoidal shape, as it can be seen in *Figure III.7*.

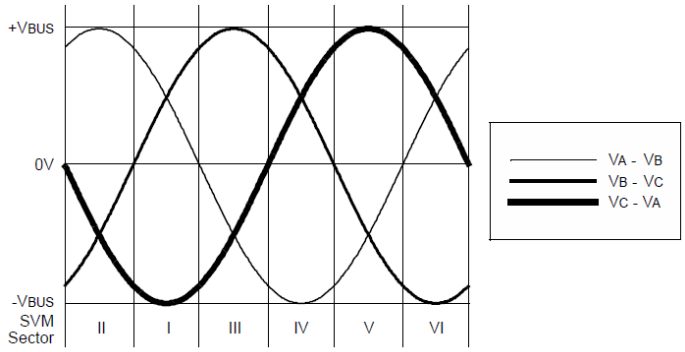

Figure III.7 Line-to-line voltage using SVM

SVM by definition has 6 commutation sectors, one for each switching vector (as in *Figure III.6*). A zoom into one of the sectors can be seen in *Figure III.8*. The thin solid line represents the voltage generated by PWM1, the dashed line - PWM2 and the thick solid line – PWM3. As SVM imposes it, centered-align PWM is used in this technique.

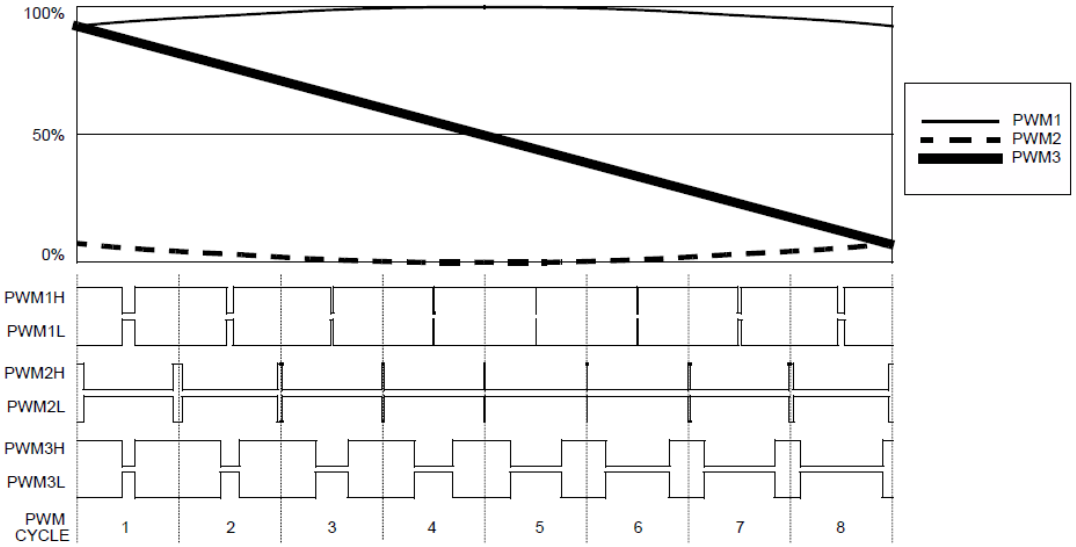

Figure III.8 Zoom into SVM commutation sector I

In *Figure III.3* the shunt resistor measures the current on the low side of the DC bus. The main advantage in doing so is that usually the low side is connected to the circuit's ground signal. This physically rejects some of the ripple. Another advantage is that differential op-amps used to measure in high-side drive can be expensive, depending on the bus voltage used. Since using low-side shunt resistor, the interest represents the state of the PWM signals on the low-side (i.e.: PWM1L, 2L, 3L). *Figure III.9* depicts a zoom on the low side signals of the PWM cycle number two from *Figure III.8*, where four sampling time windows can be distinguished: T0, T1, T2 and T3.

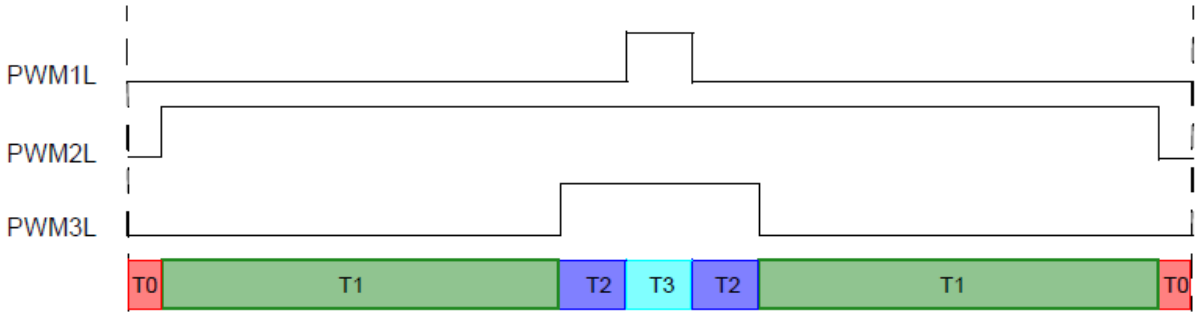

Figure III.9 Sampling time windows for measuring current

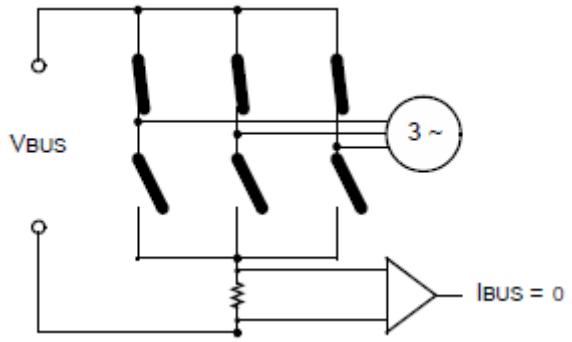

Figure III.10 No current flowing through the shunt resistor – T0

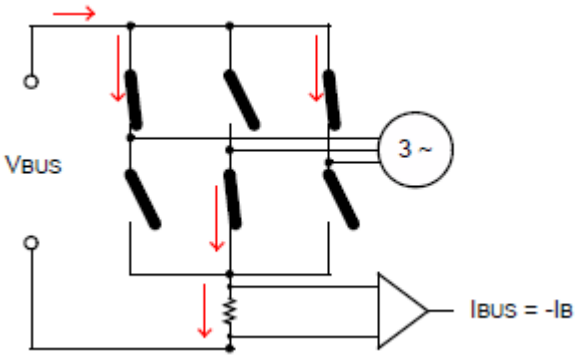

Figure III.11 Current Ib flowing through the shunt resistor – T1

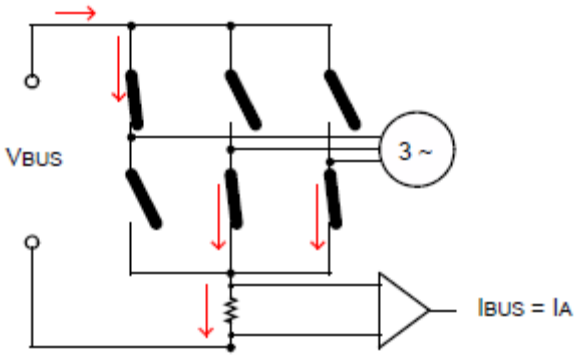

Figure III.12 Current Ia flowing through the shunt resistor – T2

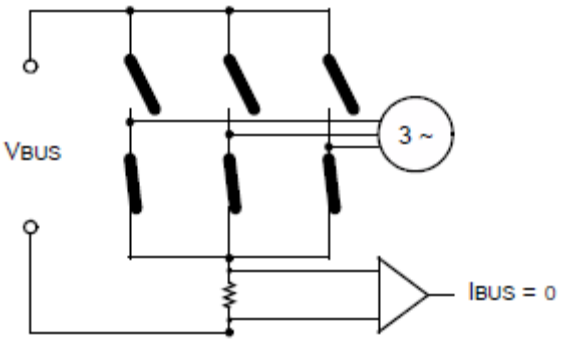

Figure III.13 No current flowing through the shunt resistor – T3

In this particular type of application, the Ic current is calculated the same as in the dual shunt scenario: $Ic = -Ia - Ib$.

However, there are several situations that single-shunt three-phase reconstruction is not possible. The first example is when the duty cycles are similar or equal, as in *Figure III.14*. T2 sampling window is too small or simply disappears.

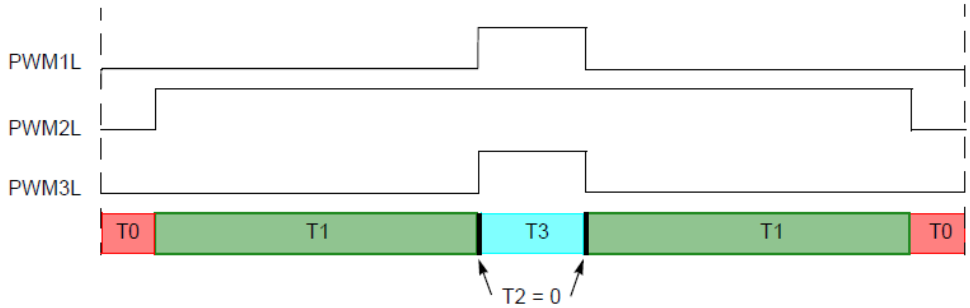

Figure III.14 Equal duty cycle current measurement

Second example is when T1 or T2 sampling windows are too small for the signal processor to be able to measure them. The next example shown in *Figure III.15* represents the sampling time windows analysis when dead time is implemented. Dead time represents the time delayed between switching off high-side MOS-FET and switching on low-side MOS-FET on the same half-bridge. This is implemented in order to prevent any shoot-throughs that might fire when the high-side MOS-FET is not fully switched off and the low-side MOS-FET is switched on.

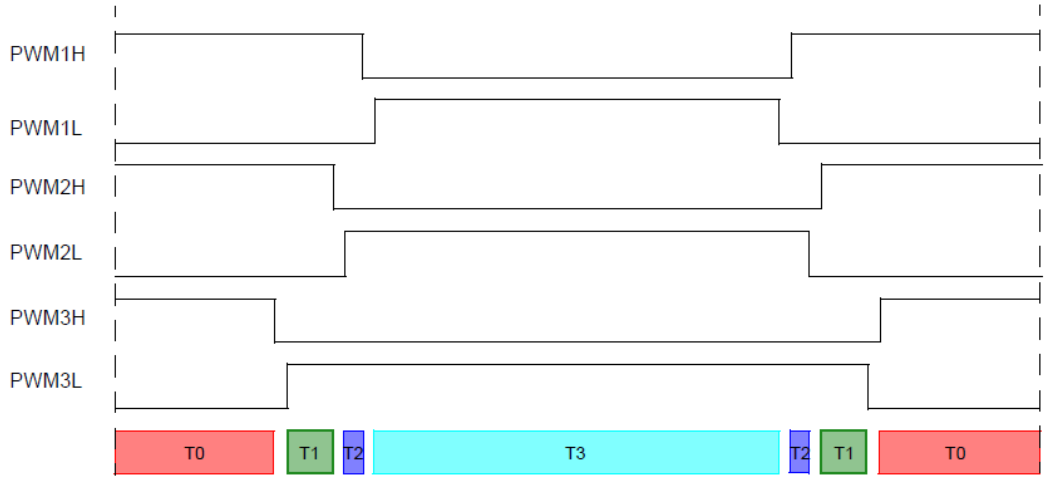

Figure III.15 Sampling time windows affected by dead time

The first problem can't be compensated for when T2=0. However, when T2 is too small for the analog circuitry to be stable but the double period of T2 is sufficient, compensation is possible by moving the right T2 period back to the left, as in *Figure III.16*.

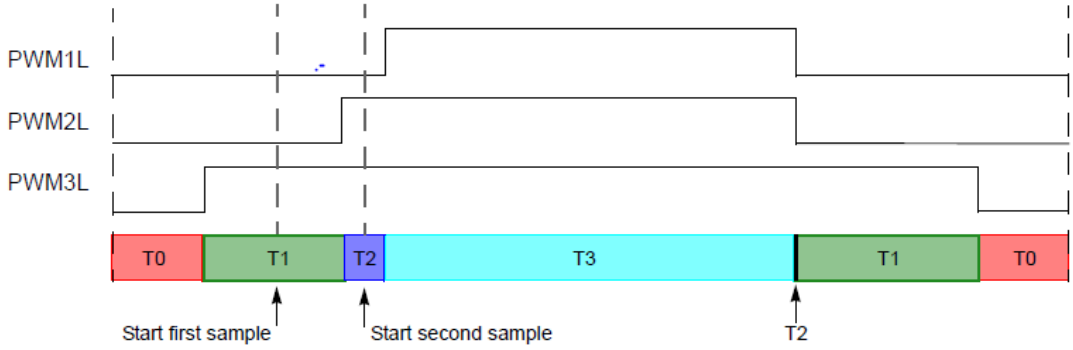

Figure III.16 T2 sampling window compensation and sampling periods

This requires more computation from the signal processor used to implement the technique, but makes single-shunt three-phase reconstruction possible with very good results.

Figure III.17 and *Figure III.18* depicts the reconstructed phase currents and reconstructed phase currents vs. the DC bus current measured by the shunt. The experimental results in which the three phase currents are reconstructed and used based on the DC bus current is depicted in *Figure III.18*.

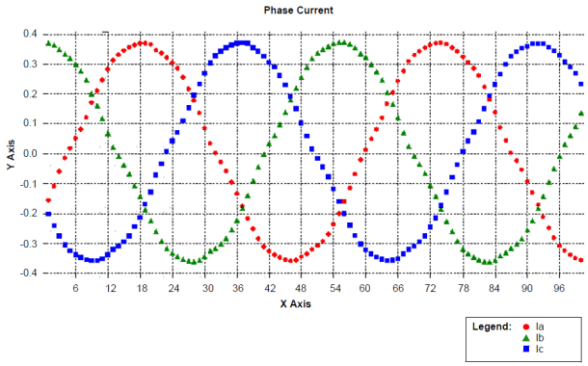

Figure III.17 Reconstructed phase currents

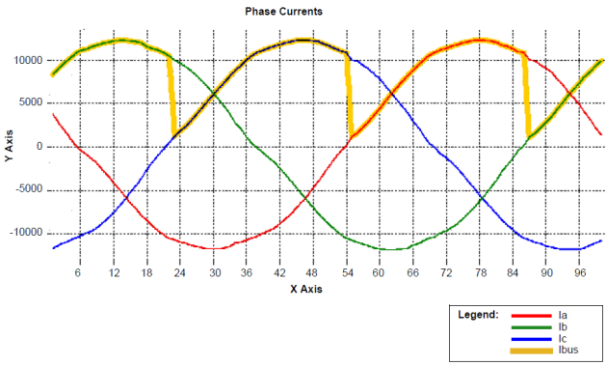

Figure III.18 Reconstructed phase currents vs. bus current

Figure III.19 represents the phase voltages generated by the SVM block described above. They have the same waveform as the theoretical phase voltages presented in *Figure III.5*.

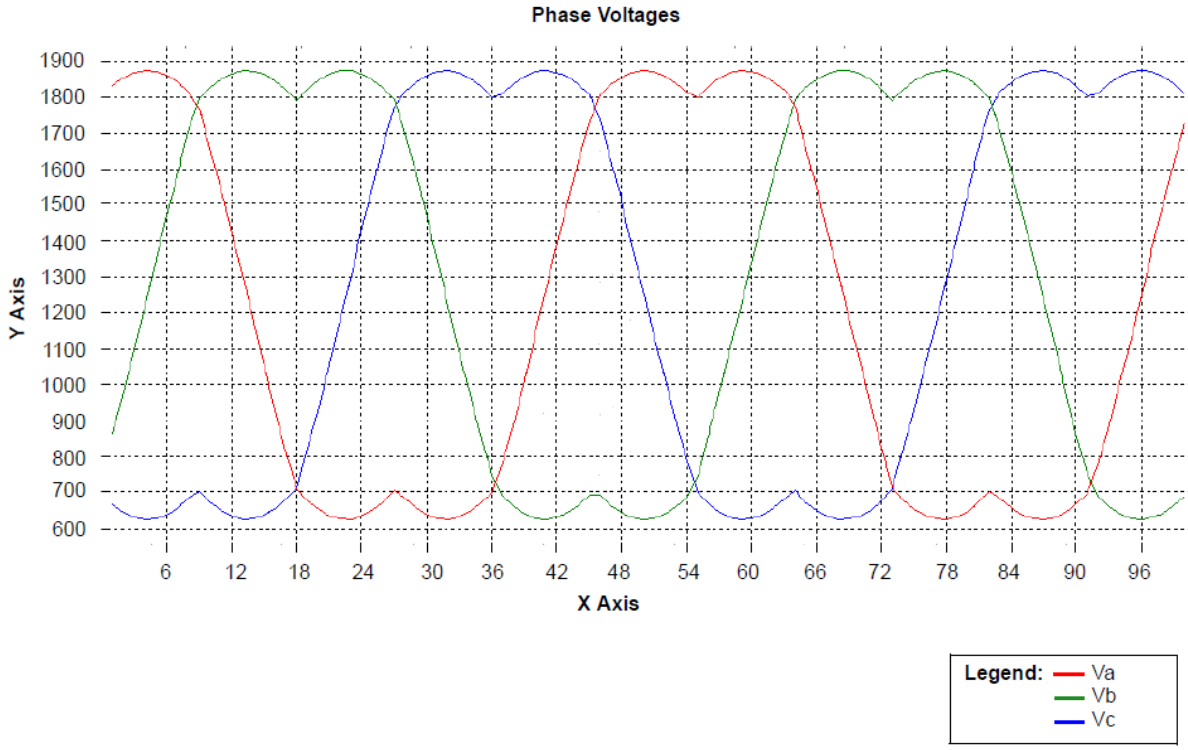

Figure III.19 Generated phase voltages

Subchapter 2 Schematics and analysis

This subchapter concentrates on implementing a cost effective, self-sufficient working circuitry to efficiently drive the blower's PMSM motor.

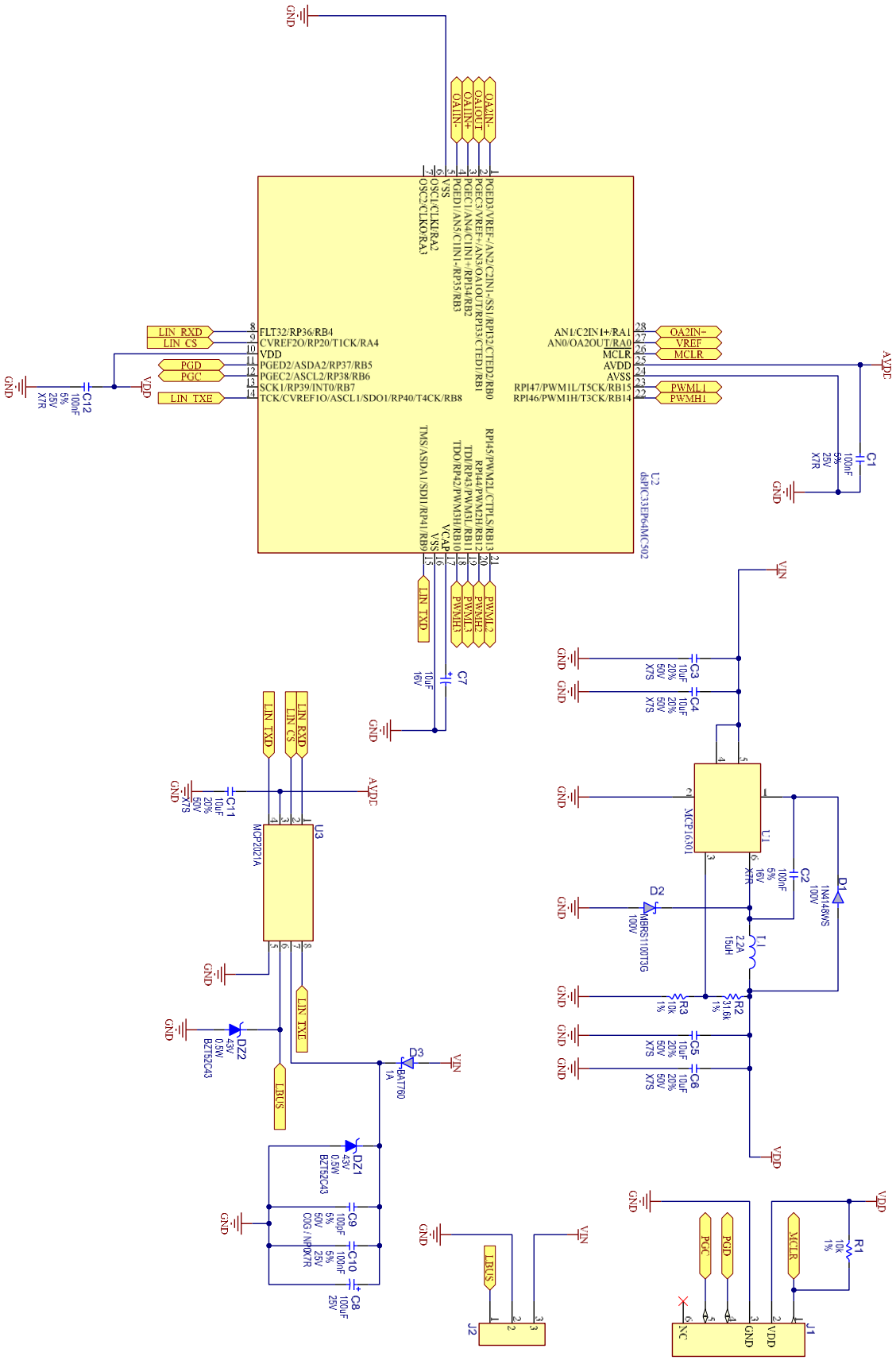

Figure III.20 PMSM controller schematic - Part 1: MCU, SMPS, LIN Transceiver, connectors

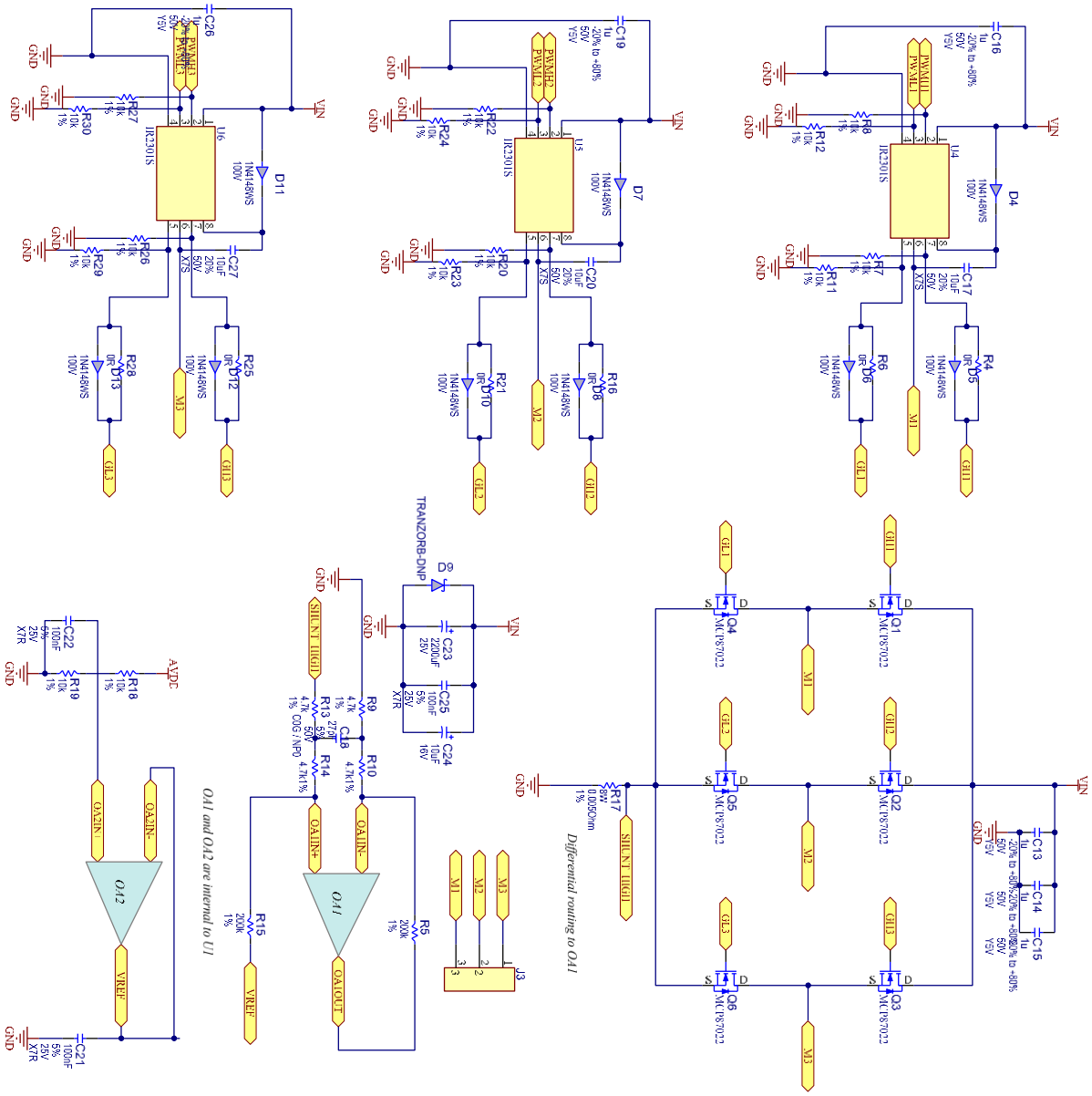

Figure III.21 PMSM controller schematic - Part 2: Op-Amps, Three-Leg Bridge, Gate Drivers

While having a look at the whole picture of the schematic, it can be split and analyzed up to sub-circuits. The main circuits that are analyzed are:

- the three-leg bridge with one gate driver
- the shunt and op-amp circuitry
- the LIN transceiver
- the Buck SMPS

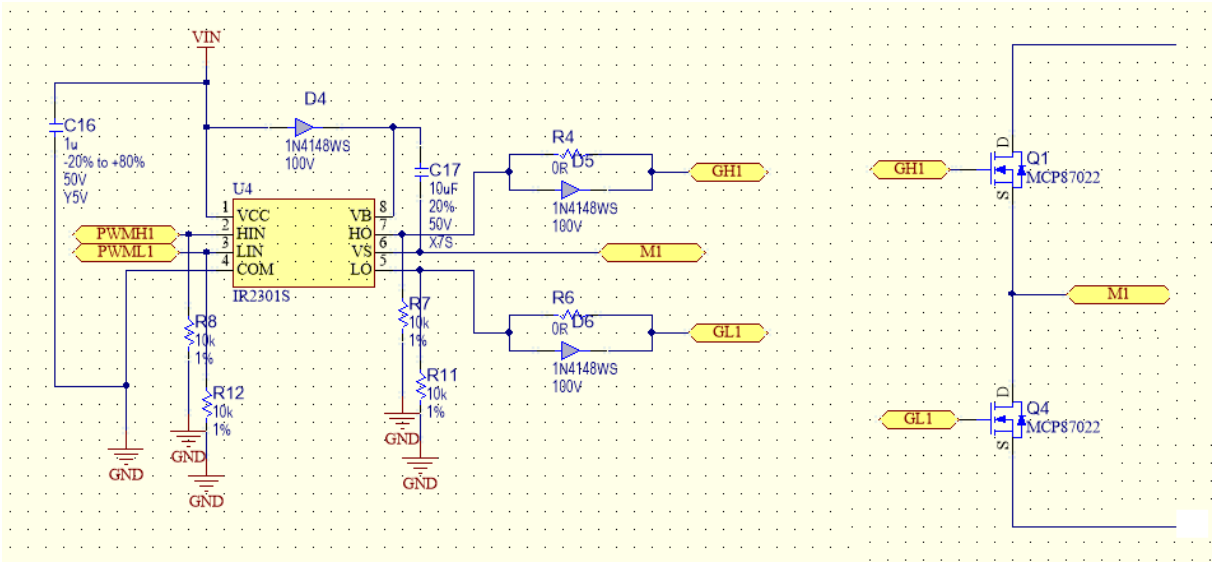

Figure III.22 One leg of the three-leg bridge, including gate driver

Figure III.22 depicts one third of the power circuitry: two N-channel MOS transistor (Q1 – high side, and Q4 – low side). Q1's source is connected to Q4's drain, and the motor phase (M1) is connected between them. U4 is a high and low side MOS-FET driver. Its input signals are PWMH1 and PWML1 and the driver outputs signals HO and LO. In order for the driver to be able to output a high current to HO pin, a bootstrap capacitor (C17) is used. Resistors R4 and R6 and diodes D5 and D6 are used to limit the current to the gate of the transistors.

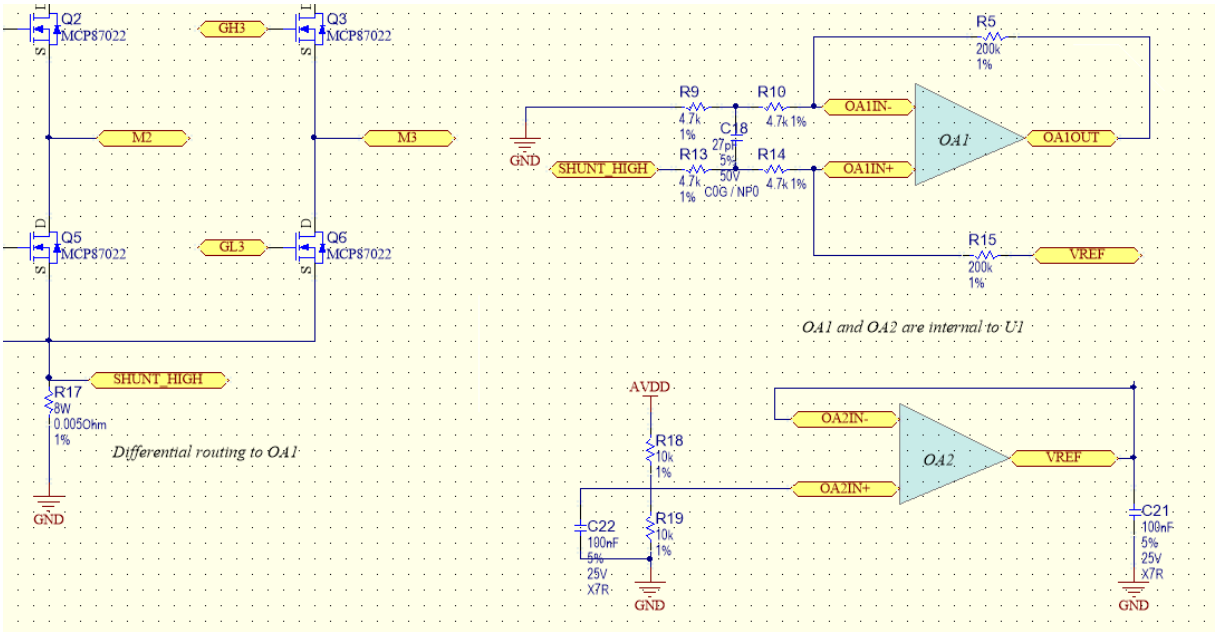

Figure III.23 Shunt and op-amp circuitry

Figure III.23 presents the 8W shunt resistor (R17 – 5 mΩ) on which the current measurement is done. OA1 and OA2 are two op-amps that are internal to the dsPIC microcontroller used to implement the single-shunt FOC algorithm. OA1 amplifies the shunt voltage with a gain of 21.2, while OA2 is used as a buffer for the reference voltage VREF (1.65V) which is used by OA1 to bias (pull-up) the shunt voltage, in order for it to be in the 0-3.3V interval required by the dsPIC's ADC converter.

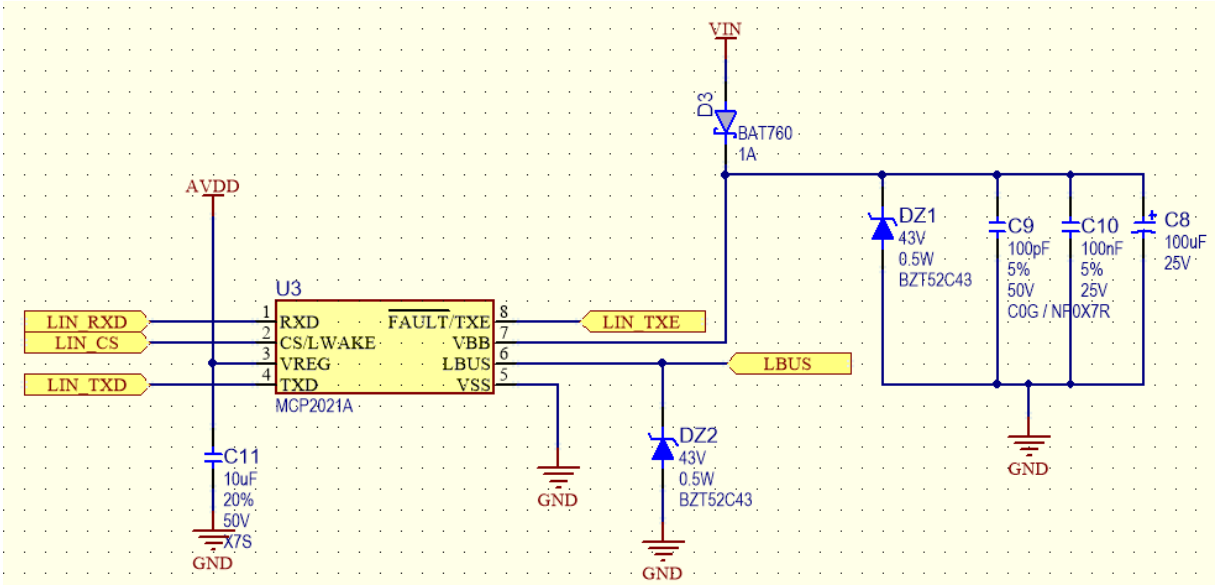

Figure III.24 LIN transceiver with integrated voltage regulator

Figure III.24 presents the MCP2021A (U2) LIN transceiver with integrated voltage regulator, and its peripheral circuitry. U3 inputs the VBB (automotive battery voltage) and the LIN bus, and outputs TTL 3.3V compatible RX and TX signals for the microcontroller. Also from the VBB it powers up the internal voltage regulator (which can provide up to 70 mA) and outputs a 3.3V voltage at the VREG pin. This voltage is used to create the analog VDD voltage (AVDD) which biases the analog circuitry for the op-amps.

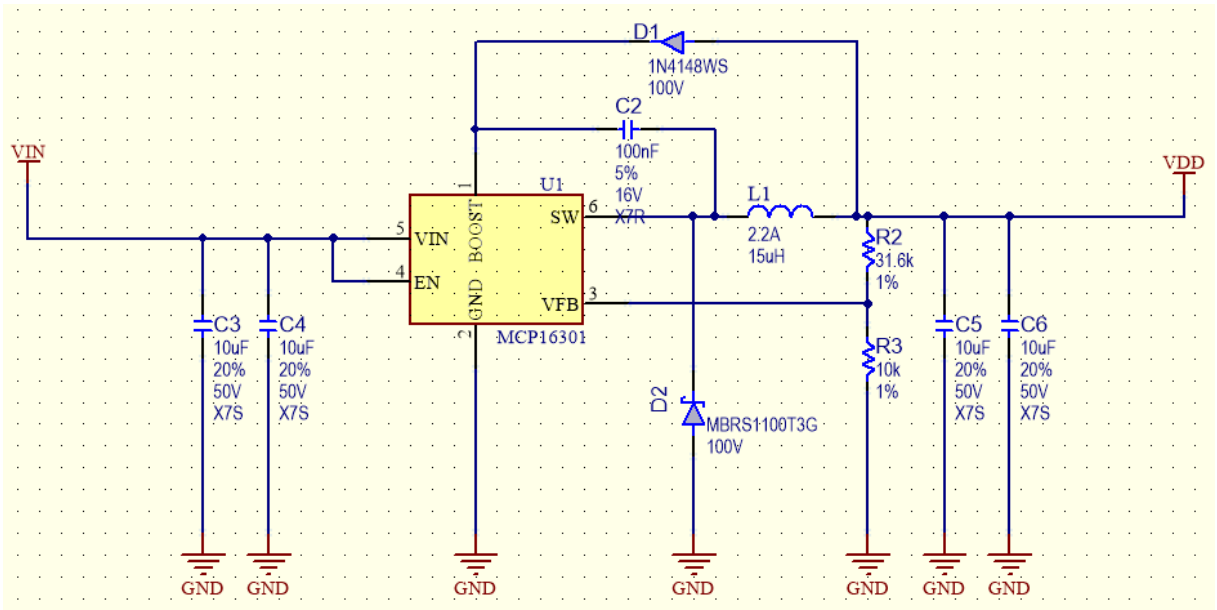

Figure III.25 Buck SMPS

The SMPS depicted in *Figure III.25* powers up the digital part of the PMSM controller (the dsPIC microcontroller). U1 chip is the MCP16301, which has a Buck topology and accepts input voltages of up to 36V, with selectable output. In this application the configured output (VDD) is 3.3V.

In *Table III.2* the auto-generated bill of materials requested for the blower motor control board.

Qty	Designator	Manufacturer	Manufacturer Part Number	Supplier	Supplier Part Number
6	C1, C10, C12, C21, C22, C25	AVX	06033C104JAT2A	Farnell	1740614
1	C2	AVX	0603YC104JAT2A	Farnell	1740612
8	C3, C4, C5, C6, C11, C17, C20, C27	TDK	C3225X7S1H106M250AB	Farnell	2309045
2	C7, C24	AVX	TCJA106M016R0200	Farnell	1658938
1	C8	PANASONIC	EEEFK1E101XP	Farnell	1850109
1	C9	MULTICOMP	MCCA000204	Farnell	1759066
6	C13, C14, C15, C16, C19, C26	MULTICOMP	MCCA000552	Farnell	1759432
1	C18	MULTICOMP	MCCA000197	Farnell	1759058
1	C23	MULTICOMP	MCGPR25V228M13X26	Farnell	1902893
10	D1, D4, D5, D6, D7, D8, D10, D11, D12, D13	MULTICOMP	1N4148WS	Farnell	1466524
1	D2	ON SEMICONDUCTOR	MBRS1100T3G	Farnell	9555862
1	D3	NXP	BAT760	Farnell	8734593
2	DZ1, DZ2	DIODES INC.	BZT52C43	Farnell	1902442
1	J1	Microchip	TC2030-MCP	microchipDirect	TC2030-MCP
1	L1	COILCRAFT	MSS6132-153MLC	Farnell	2288654
6	Q1, Q2, Q3, Q4, Q5, Q6	Microchip	MCP87022	microchipDirect	MCP87022T-U/MF
16	R1, R3, R7, R8, R11, R12, R18, R19, R20, R22, R23, R24, R26, R27, R29, R30	MULTICOMP	MCMR06X1002FTL	Farnell	2073349
1	R2	VISHAY DRALORIC	CRCW060331K6FKEA	Farnell	2138454
6	R4, R6, R16, R21, R25, R28	PANASONIC	ERJ3GEY0R00V	Farnell	2059527
2	R5, R15	MULTICOMP	MCMR06X2003FTL	Farnell	2073422

4	R9, R10, R13, R14	WELWYN	ASC0603-4K7FT5	Farnell	2078913
1	R17	BI TECHNOLOGIES/TT ELECTRONICS	BCS80R005F	Farnell	1114445
1	U1	Microchip	MCP16301T-E/CH	Farnell	MCP16301T-E/CH
1	U2	Microchip	dsPIC33EP64MC502	microchipDirect	dsPIC33EP64MC502-E/MM
1	U3	Microchip	MCP2021A	microchipDirect	MCP2021A-330E/SN
3	U4, U5, U6	IR	IR2301SPBF	Farnell	8639060

Table III.2 Blower PMSM controller board BOM

Subchapter 3 Layout

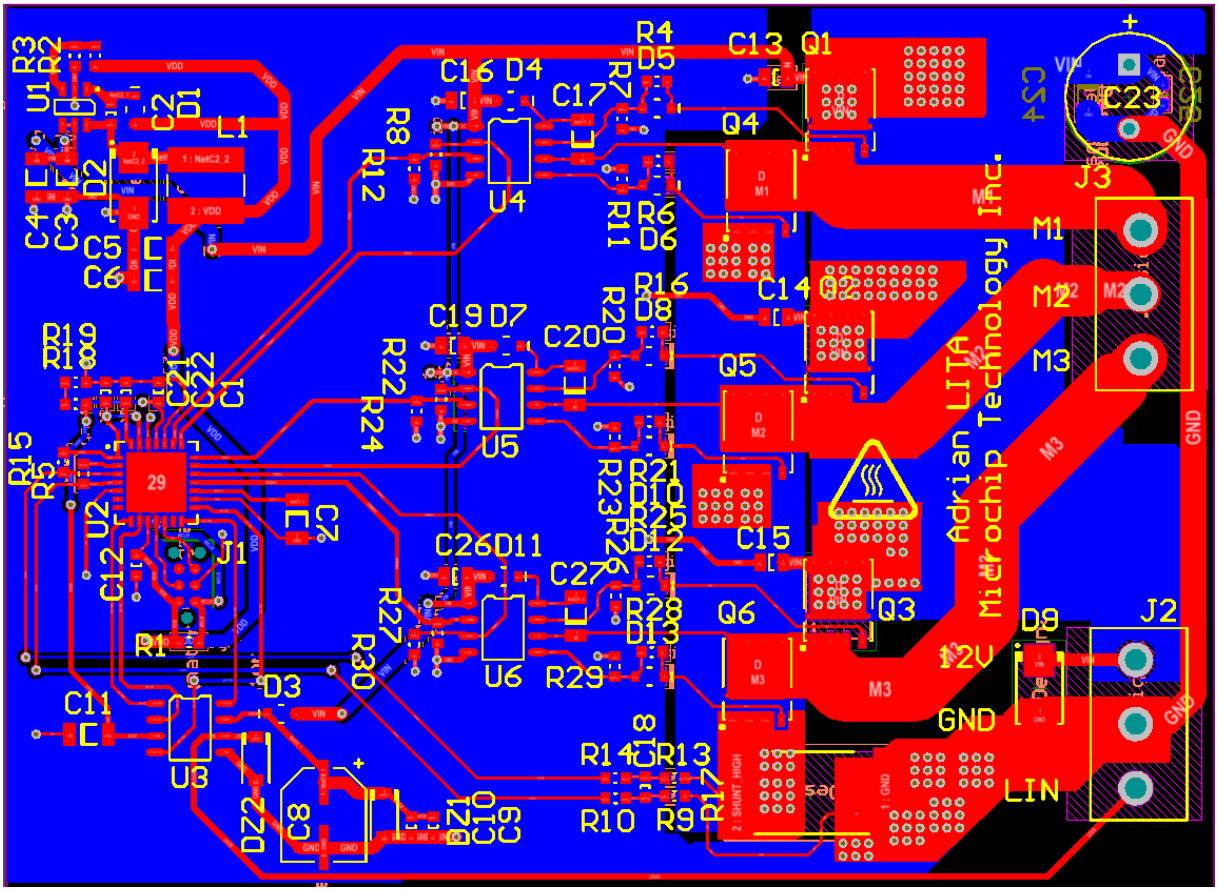

Figure III.26 PMSM controller PCB layout

In *Figure III.26* the PCB layout of the PMSM controller is displayed. In the right side of the board we have the high current circuits: battery connector (J2), motor connector (J3), the three-leg bridge (Q1, Q2, Q3, Q4, Q5 and Q6) and the power shunt (R17). Moving to the left we see the MOS-FET gate drivers (U4, U5 and U6). On the left side of the board we have the microcontroller (U2 – center), the LIN transceiver (U3) and its peripheral circuitry in the bottom and the Buck SMPS (U1) to the top.

In order to give a better perspective of the whole board, a 3D representation of it can be seen in *Figure III.27*.

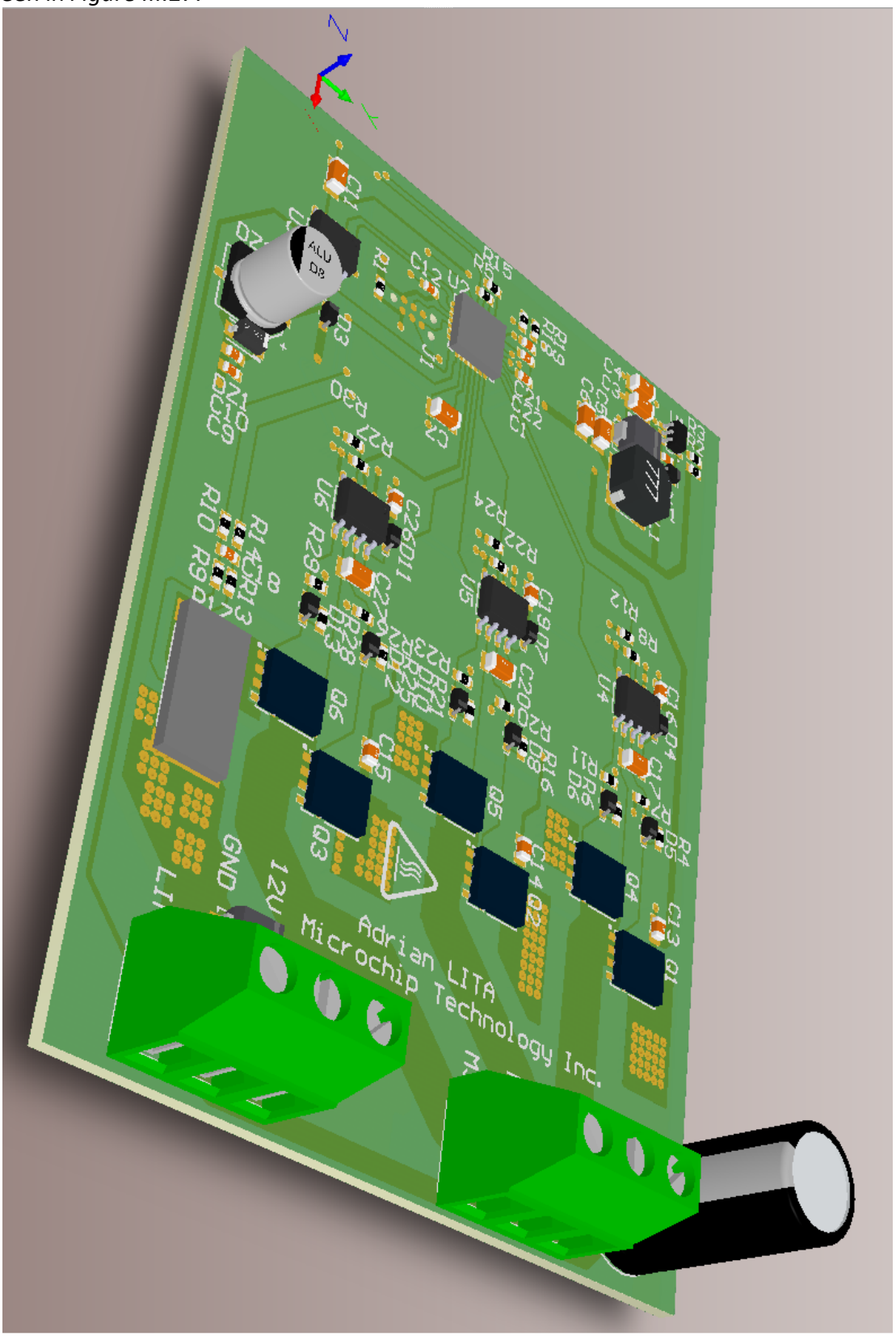

Figure III.27 3D representation of the PMSM controller board

Chapter IV. Trap door actuators

Trap doors (or air doors) are basically flaps used to allow, prevent or redirect the air flow, in order to combine fresh air, hot air and cooled air in a specific way. The air locks usually consists of a stepper motor (with or without mechanical reduction) and an I-shaped door.

They are responsible for mixing hot and cooled air together in order for a desired temperature to be achieved. They are also responsible for allowing fresh air to come into the car, or disallowing it and recirculate the air inside. Last but not least, in automatic climate control systems where the user only specifies the flow by touching buttons, they are responsible for redirecting the air to the user's desired air vent: front, legs, defrost or a mix of these.

The trap doors are usually made with stepper motors instead of other types of motors because stepper motors provide a more precise angle of movement and a higher resolution, without the need for sensors and other type of feedback, which costs.

Subchapter 1 Stepper motor control theory (13) (14)

In air-door type of applications, stepper motors have many advantages compared to other motors: fixed size of the step and great holding torque. They are also brushless motors, that don't create electrical arcs that could mean supplementary electrical noise to the car; also, if no reduction is used (i.e.: direct drive) stepper motors are usually very low noise (acoustic) motors. Due to their high torque, both stationary and rotary, they are perfect for running in direct-drive positioning systems.

There are several types of stepper motors, the most common of them being the permanent magnet motors. Based on the construction of the motors, the two most common topologies are the unipolar connection (*Figure IV.1*) and the bipolar connection (*Figure IV.2*) of the windings.

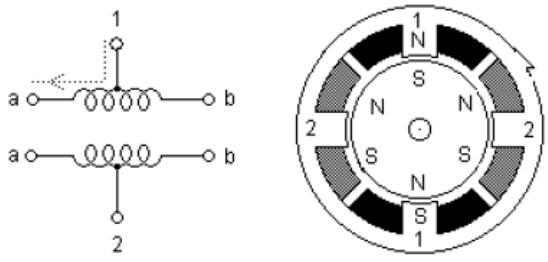

Figure IV.1 Unipolar stepper motor

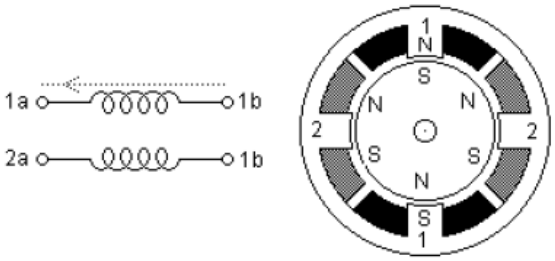

Figure IV.2 Bipolar stepper motor

The advantage of bipolar stepper motors is that instead of having the current run through half the coil, it runs through the whole coil, producing more torque for the same size. The drawback however is dictated by the complexity of the control circuitry, which will require a circuit capable of changing the polarity, such as an H-bridge.

In the present chapter bipolar stepper motors are focused, since they are the targeted motors for the current application. *Table IV.1* and *Table IV.2* represents a comparison between running the motor with only one winding energized at a time (low

consumption) and both windings energized at a time (high torque). Symbols "+" and "-" indicate the polarity of the voltage applied on the respective terminal, and "0" indicate that no voltage is applied. In both cases 12 full steps are executed.

Terminal/Step	1	2	3	4	5	6	7	8	9	10	11	12
1a	+	0	-	0	+	0	-	0	+	0	-	0
1b	-	0	+	0	-	0	+	0	-	0	+	0
2a	0	+	0	-	0	+	0	-	0	+	0	-
2b	0	-	0	+	0	-	0	+	0	-	0	+

Table IV.1 Controlling bipolar stepper motors - low consumption (wave drive)

Step/Terminal	1	2	3	4	5	6	7	8	9	10	11	12
1a	+	+	-	-	+	+	-	-	+	+	-	-
1b	-	-	+	+	-	-	+	+	-	-	+	+
2a	-	+	+	-	-	+	+	-	-	+	+	-
2b	+	-	-	+	+	-	-	+	+	-	-	+

Table IV.2 Controlling bipolar stepper motors - max torque (two-phase on)

In stepper motor theory there is another concept called half-stepping, which can be derived into a more complex concept called micro-stepping. Stepper motors have a fixed number of steps for every mechanical revolution, all steps usually being equal to each other, and the step size is dictated by the way the windings and magnets are placed inside the motor (physically). Half-stepping technique makes possible the movement of the rotor only one half of the step. In addition, micro-stepping represents halving the halves – after half-stepping is implemented, another half-stepping method is implemented of the new one, resulting in quarter-step stepping, and so on (*Figure IV.3*). Micro-stepping in general is a technique used not only to obtain more steps and precision from a stepper motor, but to lower the current ripple and harmonics the motor needs when executing a high number of steps. In the current application micro-stepping is not used since trap door applications do not require such precision, and the ripple is low because the current is low. However, half-stepping will be implemented, and the control sequence is presented in *Table IV.3*. To be noted that the mechanical movement in both *Table IV.2* and *Table IV.3* is the same: 12 full-steps equals the same rotation as 24 half-steps. Half-stepping combines wave-drive with two-phase on.

Half-Step/Terminal	01	02	03	04	05	06	07	08	09	10	11	12	13	14	15	16	17	18	19	20	21	22	23	24
1a	+	+	0	-	-	-	0	+	+	+	0	-	-	-	0	+	+	+	0	-	-	-	0	+
2b	-	-	0	+	+	+	0	-	-	-	0	+	+	+	0	-	-	-	0	+	+	+	0	-
2a	0	+	+	+	0	-	-	-	0	+	+	+	0	-	-	-	0	+	+	+	0	-	-	-
2b	0	-	-	-	0	+	+	+	0	-	-	-	0	+	+	+	0	-	-	-	0	+	+	+

Table IV.3 Controlling bipolar stepper motors - half stepping

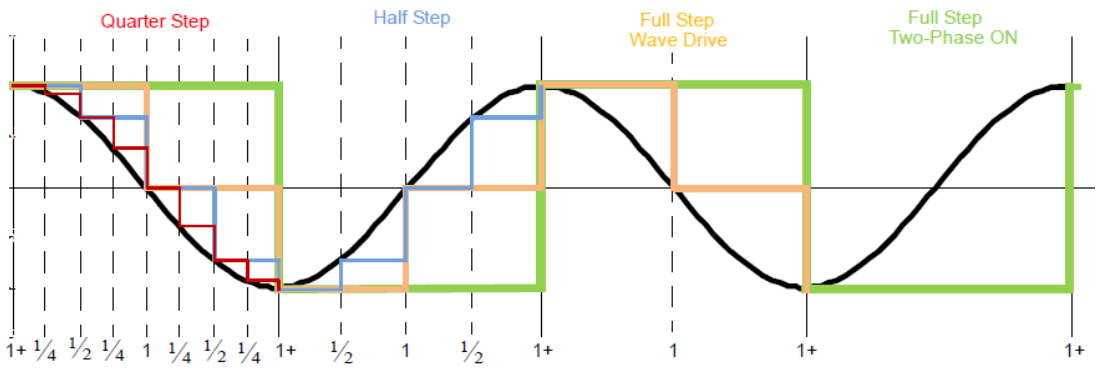

Figure IV.3 Micro-stepping generation

In order to achieve the trap door functionality, having a stepper motor requires positioning it to a certain angle. When positioning, the motor should be moved from one angle to another. This implies accelerating the motor, holding it under constant speed and then decelerating it. Accelerating a stepper motor should not be done in faster than the rated acceleration (specified by datasheet) or otherwise the rotor will stall or fail to start.

Subchapter 2 Schematics and analysis

The schematic presented in this subchapter is able to drive bipolar stepper motors. It will be presented and explained in detail further on.

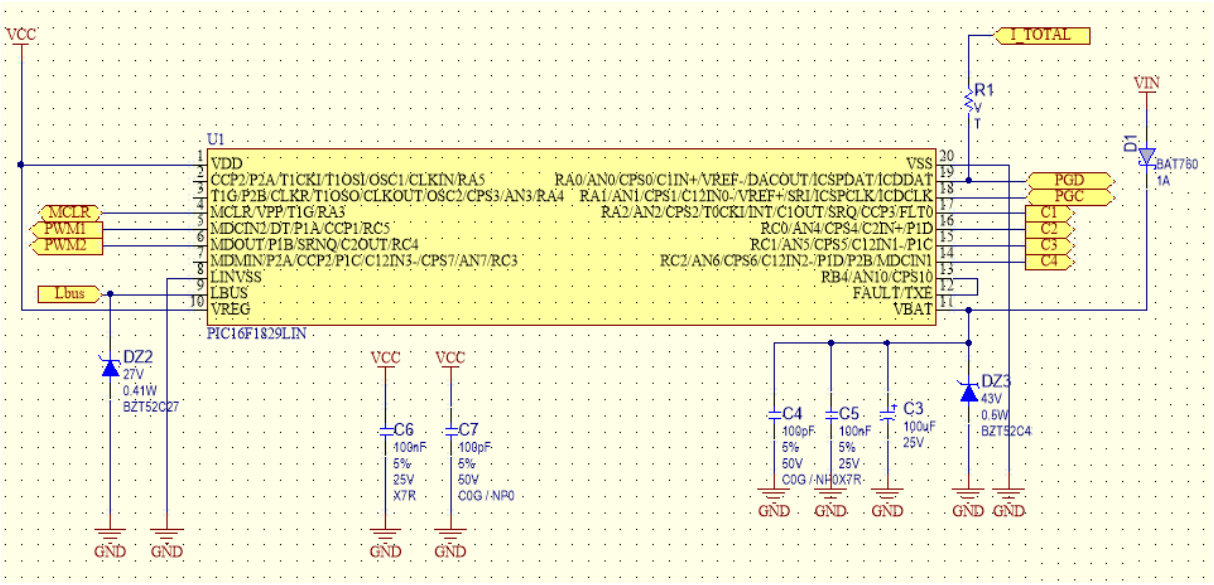

Figure IV.4 Stepper motor driver – Part 1: microcontroller with integrated LIN transceiver and voltage regulator

Figure IV.4 depicts the PIC16F1829LIN (U1) microcontroller with integrated LIN transceiver and voltage regulator. The input voltage, received from the automotive battery is VIN, which goes to VBAT pin of U1. This is internally regulated, and the output of 5V (VCC) resides on VREG pin. VCC is used to power up both the digital and the analog part, including U1 itself.

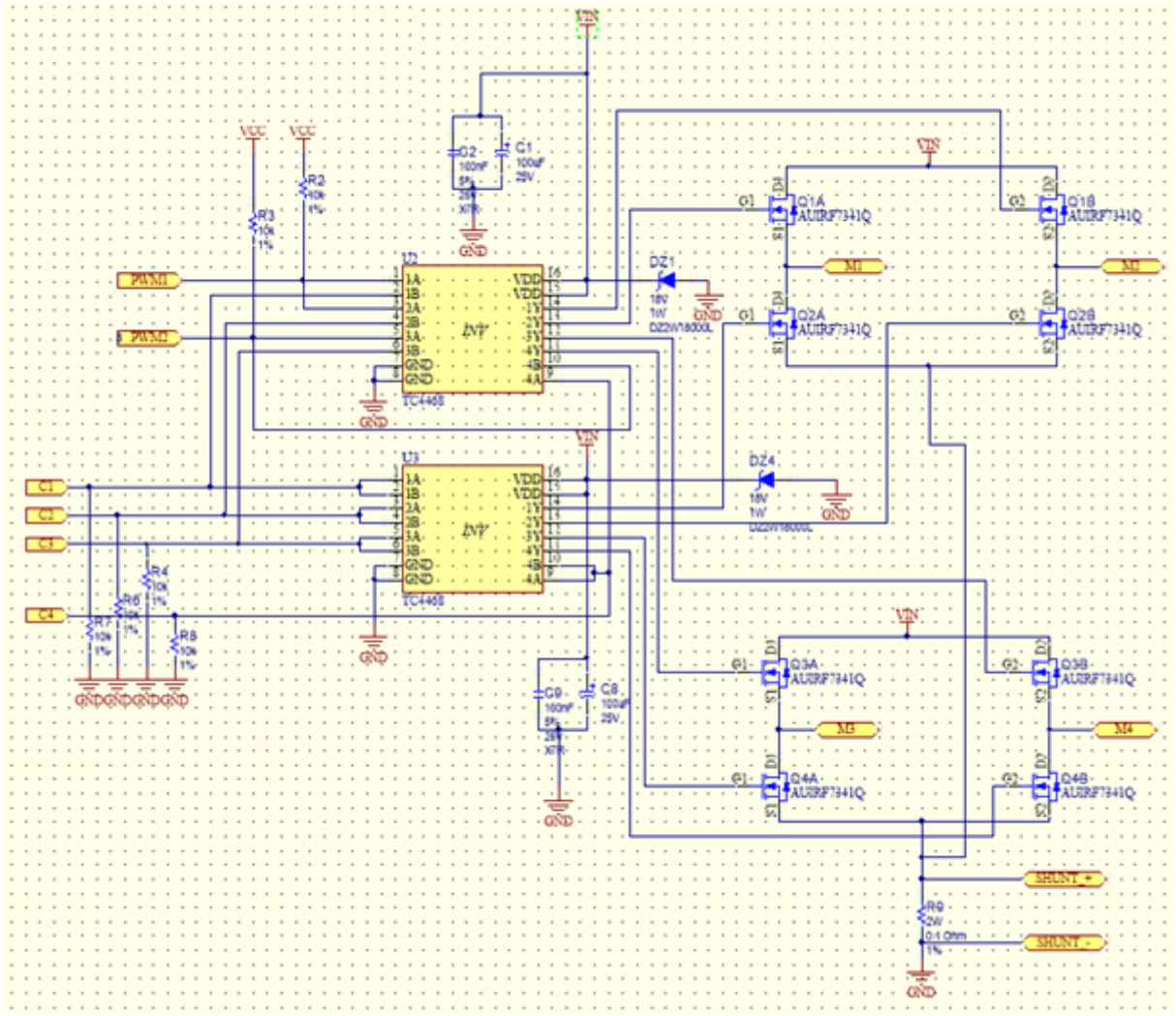

Figure IV.5 Stepper motor driver – Part 2: gate drivers, MOS-FETs and measurement shunt resistor

Figure IV.5 depicts two gate drivers: U2 and U3 (TC4468) which are able to directly control the two H-bridges made of N-channel automotive MOS-FETs. The power plan of the board is designed to work with automotive stepper motors up to 2A. The MOS-FETs are encapsulated in 4 SOIC-8 packages: 2 x N-channel MOS-FETs per package. The total current that is driven through the two coils of the stepper motor is measured using the R9 shunt resistor (100 mΩ - 2W).

The advantage of the TC446x gate drivers is that they can be powered directly from the battery, with no need for power conversion.

M1, M2, M3 and M4 are the connections to the stepper motor. M1 and M2 connect one winding, and M3 and M4 connect the second winding.

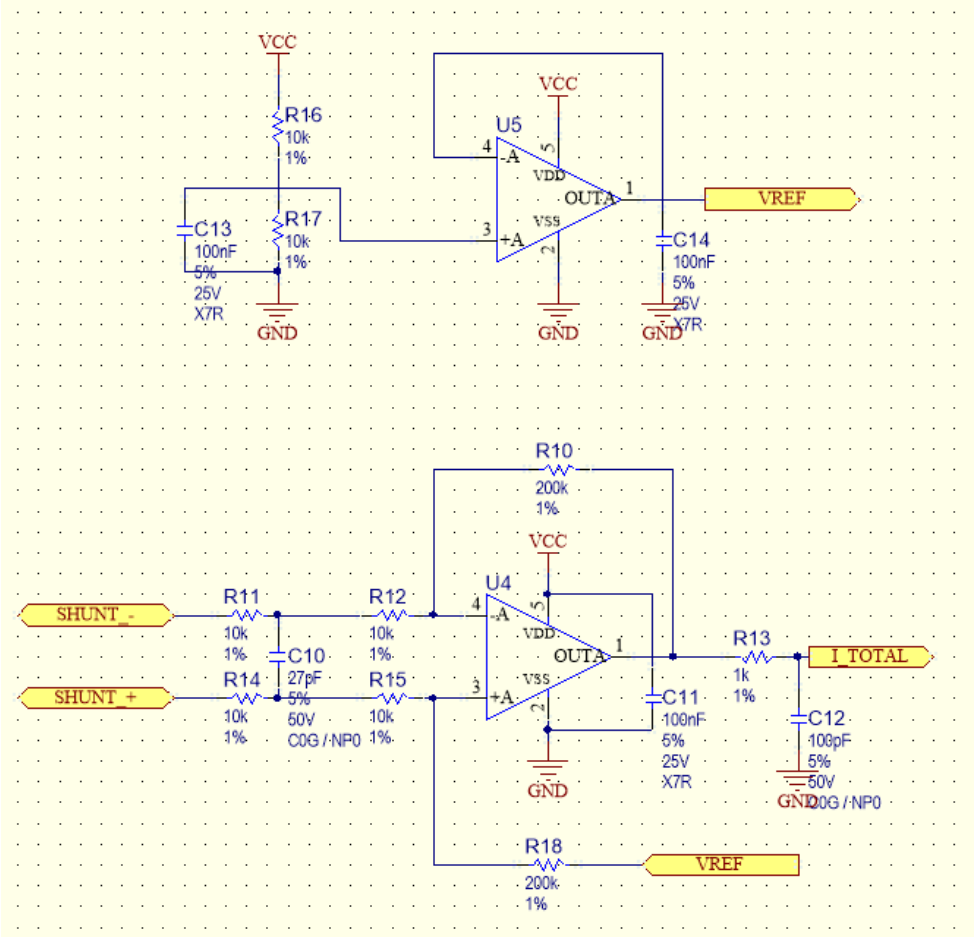

Figure IV.6 Stepper motor driver – Part 3: current measurement circuitry

In *Figure IV.6* there are the two op-amps (MCP6021) used for amplifying the voltage measured on the shunt. U5 is a buffer for VREF (2.5V) which biases the U4 op-amp. U4 amplifies the shunt voltage having an output that will be read by the microcontroller's (U1) analog to digital converter (ADC – I_TOTAL).

Table IV.4 presents the auto-generated bill of materials for this board. Farnell was chosen as the primary supplier for discrete components. microchipDirect provided all Microchip's parts.

Qty	Designator	Manufacturer	Manufacturer Part Number	Supplier	Supplier Part Number
3	C1, C3, C8	PANASONIC	EEEFK1E101XP	Farnell	1850109
7	C2, C5, C6, C9, C11, C13, C14	AVX	06033C104JAT2A	Farnell	1740614
3	C4, C7, C12	MULTICOMP	MCCA000204	Farnell	1759066
1	C10	MULTICOMP	MCCA000197	Farnell	1759058
1	D1	NXP	BAT760	Farnell	8734593
2	DZ1, DZ4	PANASONIC	DZ2W18000L	Farnell	2285376
1	DZ2	MULTICOMP	BZT52C27	Farnell	1466568
1	DZ3	DIODES INC.	BZT52C43	Farnell	1902442
1	J3	PHOENIX	1725672	Farnell	3041414

		CONTACT			
4	Q1, Q2, Q3, Q4	IRF	AUIRF7341Q	Farnell	1909585
13	R2, R3, R4, R5, R6, R7, R8, R11, R12, R14, R15, R16, R17	MULTICOMP	MCMR06X1002FTL	Farnell	2073349
1	R9	BOURNS	CRM2010-FX-R100ELF	Farnell	1865260
2	R10, R18	MULTICOMP	MCMR06X2003FTL	Farnell	2073422
1	R13	MULTICOMP	MCMR06X1001FTL	Farnell	2073348
1	U1	Microchip	PIC16F1829LIN	microchipDirect	PIC16F1829LIN-E/SS
2	U2,U3	Microchip	TC4468EOE	microchipDirect	TC4468EOE
2	U4, U5	Microchip	MCP6021T-E/OT	microchipDirect	MCP6021T-E/OT

Table IV.4 Stepper motor driver BOM

Subchapter 3 Layout

The layout structure presented in *Figure IV.7* is designed to drive automotive (12V) stepper motors of up to 2A.

The left side is the microcontroller (U1) side, and on the bottom side (J2) the ICSP debug connector is present. The two quad-gate drivers are placed in the middle of the board, while the 8 MOS-transistors reside on the right side of the board.

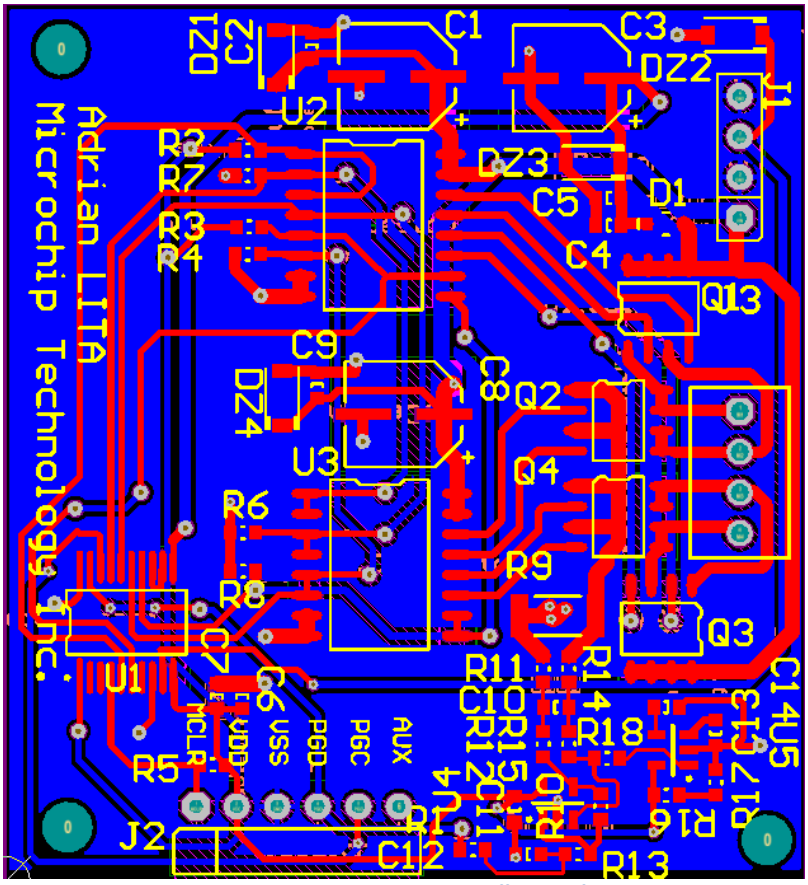

Figure IV.7 Stepper motor controller PCB layout

To give a better understanding of the placement and layout, presents the 3D representation of the controller.

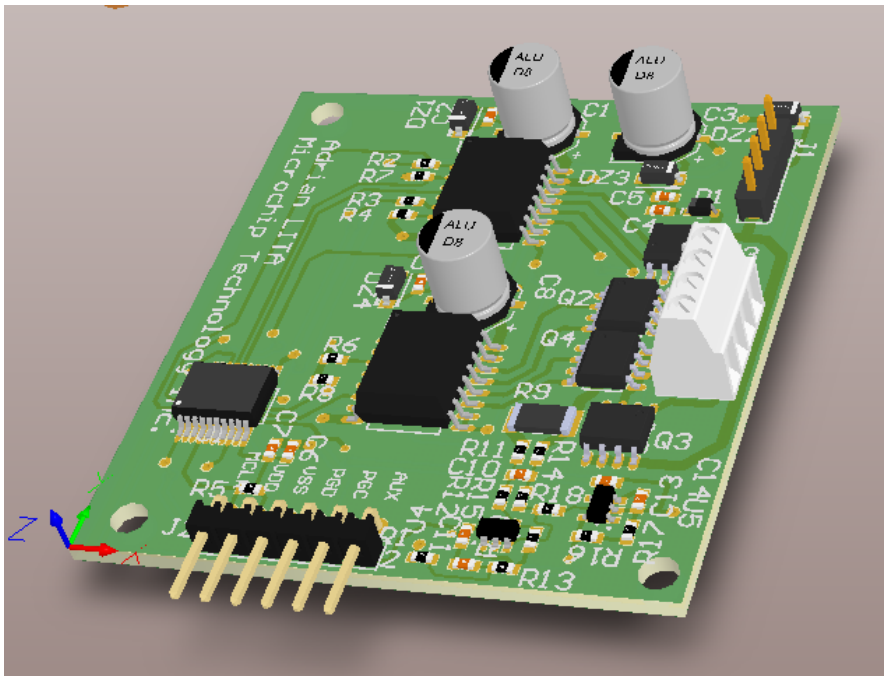

Figure IV.8 Stepper motor controller 3D representation

Chapter V. Main control unit

The main control unit can also be called climatic/climate computer. It is the part responsible for getting all the information from the user (inputs – desired temperatures for each zone, desired air flow, desired air dispensing doors), all the information from the sensors (inputs – current measured temperatures), computes the next steps, and then sends the commands to the actuators (outputs – blower motor, trap doors, air conditioning motor, etc.).

As can be seen in *Figure V.1*, the role of the main control unit (in this example – controller) is to compute the output command to the actuators, based on the input fed by the sensors, in an optimal amount of time. The optimal amount of time refers to the minimum interval of time since the user sets the desired temperature to the moment the temperature inside (basically, the temperature measured by the sensors) is achieved.

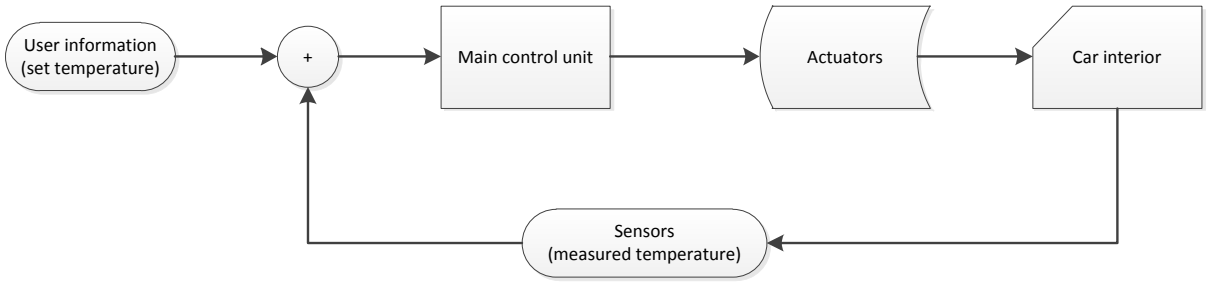

Figure V.1 Automatic climate control

In order to be functional, the main controller unit needs to do the following tasks, presented onto their own block functionality:

1. Read the user information – CAN block
2. Read the sensors – LIN block 1 and 2
3. Compute the information to be sent to the actuators – Controller block
4. Write the computed output to the actuators – LIN block 1 and 2

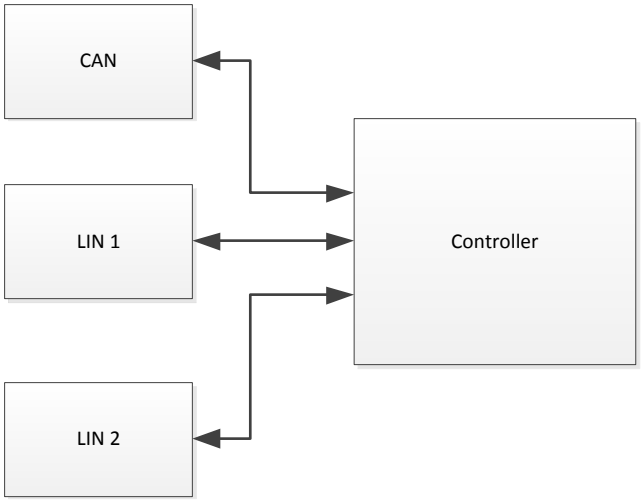

Figure V.2 Main control unit

While the CAN and LIN blocks are well described in previous chapters and have little importance here (serves as means of communication between the sensors, controller and actuators), the controller block is the core of the climatic computer. The main function of the controller is to generate a command (output) in order to bring the temperature as close as

possible to the desired value, based on a reference value (user set temperature) and a measured value (sensor measured temperature). There are several approaches in implementing such a controller:

- P controller;
- PI controller;
- PID controller;
- Fuzzy logic;
- etc.

In the present paper, a controller based on Fuzzy logic is used.

Subchapter 1 Signaling and data buses

The standard capability of the LIN Bus is to have one master and up to 16 slaves on a single bus. When doing a simple listing of the total number of devices for the 4-zone HVAC system, we have (at least) the following:

- 1 blower motor
- 1 electric AC compressor
- 1 trap door for fresh air (see *Figure I.2*)
- 1 trap door for recirculated air
- 1 trap door: charcoal filter activation
- 3 trap doors for front outlets: defroster outlet, driver outlet and passenger outlet
- 4 zones x 1 trap door for footwell outlet
- 4 zones x 1 temperature sensor
- 4 zones x 1 temperature actuator (stepper motor)
- 1 back window defroster

The total number of LIN-connected devices in this case is 21, which exceeds 16. This is the main concern for having two LIN buses in the system. The way LIN buses were thought of is to have one bus for the 4-zone specific devices, and one bus for operating the system.

LIN Bus 1:

- 1 blower motor
- 1 electric AC compressor
- 1 trap door for fresh air
- 1 trap door for recirculated air
- 1 trap door for the charcoal filter activation
- 11 nodes free for enhancements (see *Figure I.2*, *Figure I.3* and *Figure I.4*)

LIN Bus 2:

- 3 trap doors for front outlets: defroster outlet, driver outlet and passenger outlet
- 4 zones x 1 trap door for footwell outlet
- 4 zones x 1 temperature sensor
- 4 zones x 1 temperature actuator
- 1 back-window defroster

Since bus 2 has no free nodes remaining for further enhancements, they can be implemented on either the temperature sensor, or on the temperature actuator. Note that

the temperature actuator is just a mechanical valve actuated by a stepper motor, which allows more or less heat to go through the radiator, controlling the output temperature. When there is need for extra nodes on LIN bus 2, the two actuators – temperature actuator and footwell outlet trap door – can be moved on the same circuit, sharing the same LIN address. Of course, this is just one example, one can think of many other. The most radical solution would be adding the third LIN bus.

Regarding the CAN bus, as mentioned earlier, CAN is used to communicate with the dashboard, in order to interact with the user. The main controller is linked to the car's CAN bus, together with one or two extra nodes:

- Main dashboard (for driver and passenger)
- Rear panel (for rear passengers)

Rear panel is optional, since all climatic changes can be done from the main dashboard. However, for ergonomically reasons, the rear panel is present on all vehicles which have 4-zone climate system.

Subchapter 2 Control theory and Fuzzy logic

As mentioned in the beginning of the chapter, many control algorithms can be applied for temperature control. The classic PID controller would do an excellent job in temperature control. However, since its introduction in 1965, fuzzy logic got more and more notoriety in control theory. The present paper uses fuzzy logic to implement the temperature controller.

Fuzzy logic offers an alternative to the classic, binary logic (true or false), by moving the thresholds and allowing a state that is at both times true, and false – depending on how you look at it. The following example illustrates this concept: empty and full concepts of a 100 ml glass. When the glass has 0 ml of liquid in it, we can assume it's empty (thus, 0), and when the glass contains 100 ml of liquid, it is full (thus, 1). When the glass contains 30 ml of liquid, it is 70% empty and 30% full. The emptiness or fullness of the glass is then subjective, depending on the observer: one may say the glass is empty, one may say it's not. Another example (15), which is temperature based, is well pointed out by Wikipedia: a temperature measurement for anti-lock brakes might have several separate membership functions defining particular temperature ranges needed to control the brakes properly. Each function maps the same temperature value to a truth value in the 0 to 1 range. These truth values can then be used to determine how the brakes should be controlled.

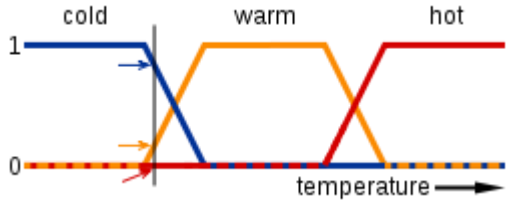

Figure V.3 Fuzzy logic temperature (15)

In *Figure V.3*, the meanings of the expressions cold, warm, and hot are represented by functions mapping a temperature scale. A point on that scale has three "truth values"—one for each of the three functions. The vertical line in the image represents a particular temperature that the three arrows (truth values) gauge. Since the red arrow points to zero, this temperature may be interpreted as "not hot". The orange arrow (pointing at 0.2) may describe it as "slightly warm" and the blue arrow (pointing at 0.8) "fairly cold".

Another good example for using fuzzy logic is with calculating the tip in a restaurant. Rules for such a problem include “if the service is poor or the food is not good, then tip is small”, “if the service is good, then the tip is average” and “if the service is excellent or the food is delicious, then the tip is high”. All these rules don’t exclude each other, so there’s no “else” statement in between them. So considering a small tip of 5%, an average tip of 10% and a generous tip of 15%, an output example for delicious food and poor service would be somewhere between 5% and 15%. For average service and delicious food, the output is between 10% and 15%. The exact output value depends on how the fuzzy controller’s parameters are set.

Using fuzzy logic a complex, highly soliciting (in terms of processor needs) algorithm can be easily be replaced by simple IF-THEN commands. The total commands are dependent on the number of output options, and there should never be an “ELSE” statement.

Subchapter 3 Schematics and analysis

First of all, in order to operate, the circuit needs to be powered. The main power supply (automotive battery – 12V) is supplied to the board. The 12V voltage (VIN) is then converted into two separate voltages: 3.3V or the microcontroller and 5V for the CAN transceiver. Since the CAN transceiver does not require a lot of current, a simple LDO is used to provide power to it. For the 3.3V signal, it is converted using a Buck converter. They are both presented in *Figure V.4*.

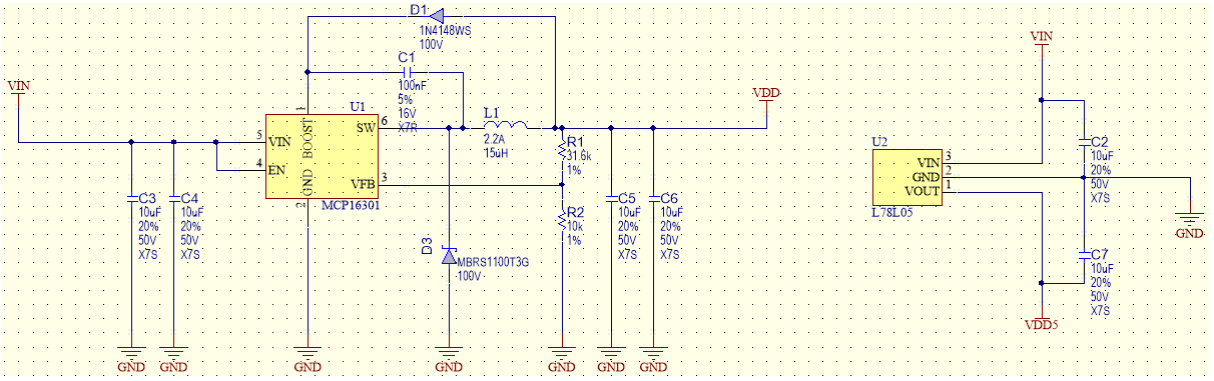

Figure V.4 Main control unit power conversion

In *Figure V.5* the transceivers used for CAN and LIN communication are presented.

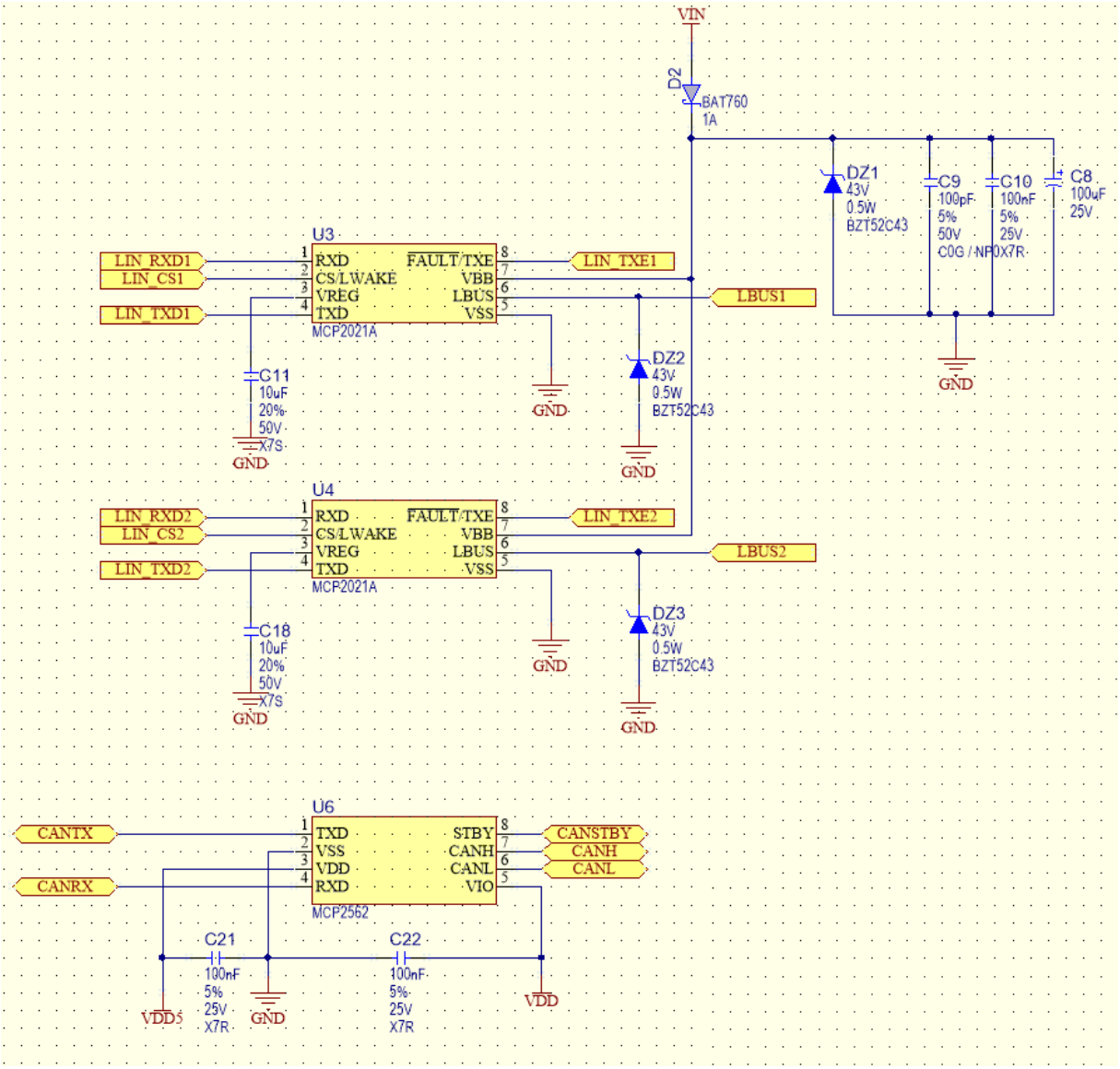

Figure V.5 CAN and LIN transceivers

The central part in the board is the microcontroller (*Figure V.6*). PIC32MX775F256H is used due to its superior processing speed and integrated communication peripherals. Without the use of external modules (only the standard transceivers), this microcontroller offers support for both LIN and CAN, while providing up to 120 MIPS of 32-bit signal processing.

For debug purposes a supplementary UART interface is used, which also acts as the active interface for Bluetooth communication with the computer.

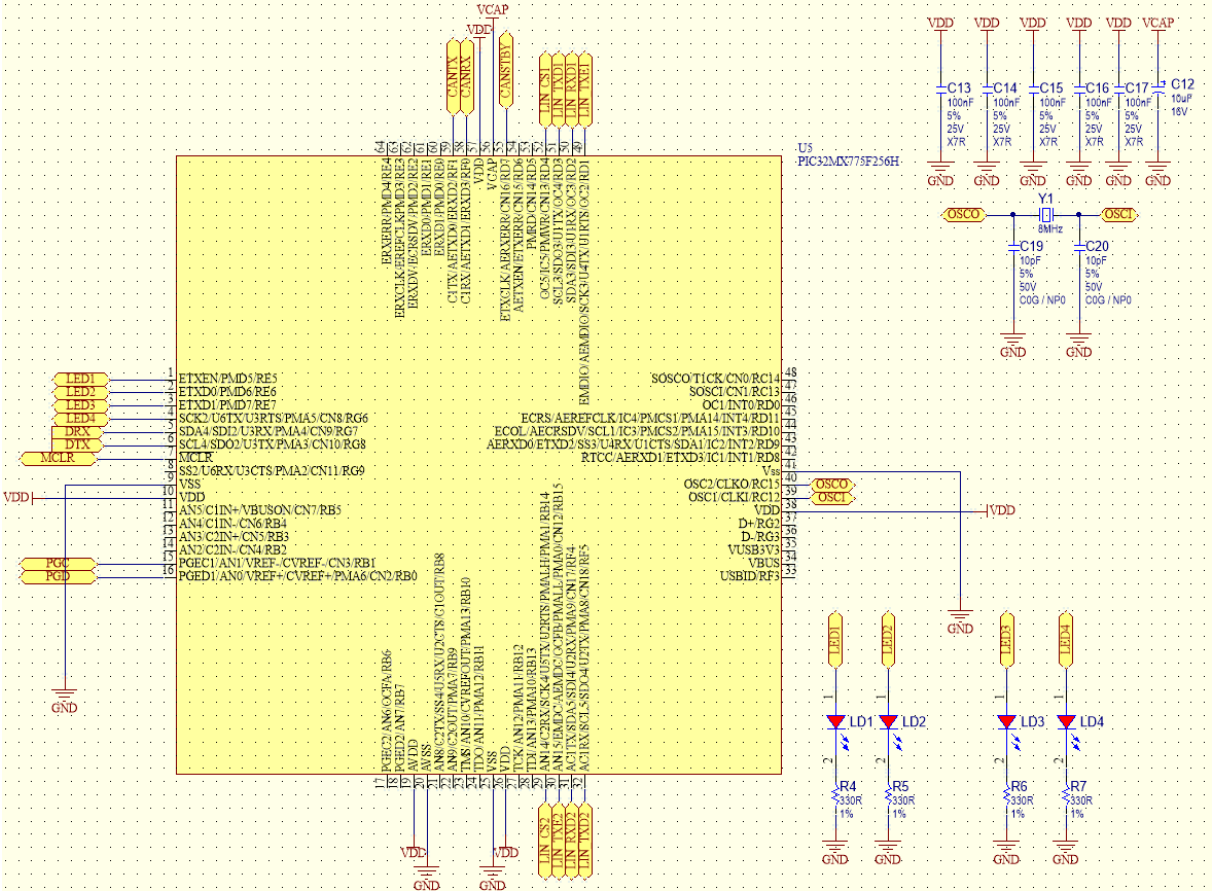

Figure V.6 Climate computer microcontroller

Table IV.4 presents the auto-generated bill of materials for this board. Farnell was chosen as the primary supplier for discrete components, and microchipDirect for Microchip-provided components.

Qty	Designator	Manufacturer	Manufacturer Part Number	Supplier	Supplier Part Number
1	C1	AVX	0603YC104JAT2A	Farnell	1740612
8	C2, C3, C4, C5, C6, C7, C11, C18	TDK	C3225X7S1H106M250AB	Farnell	2309045
1	C8	PANASONIC	EEEFK1E101XP	Farnell	1850109
1	C9	MULTICOMP	MCCA000204	Farnell	1759066
8	C10, C13, C14, C15, C16, C17, C21, C22	AVX	06033C104JAT2A	Farnell	1740614
1	C12	AVX	TCJA106M016R0200	Farnell	1658938
2	C19, C20	MULTICOMP	MCCA000192	Farnell	1759053
1	D1	MULTICOMP	1N4148WS	Farnell	1466524
1	D2	NXP	BAT760	Farnell	8734593
1	D3	ON SEMICONDUCTOR	MBRS1100T3G	Farnell	9555862

3	DZ1, DZ2, DZ3	DIODES INC.	BZT52C43	Farnell	1902442
3	J2, J3, J4	PHOENIX CONTACT	1725672	Farnell	3041414
1	L1	COILCRAFT	MSS6132-153MLC	Farnell	2288654
4	LD1, LD2, LD3, LD4	KINGBRIGHT	KPT-1608EC	Farnell	2099221
1	R1	VISHAY DRALORIC	CRCW060331K6FKEA	Farnell	2138454
2	R2, R3	MULTICOMP	MCMR06X1002FTL	Farnell	2073349
4	R4, R5, R6, R7	MULTICOMP	MCMR06X3300FTL	Farnell	2073472
1	U1	Microchip	MCP16301T-E/CH	Farnell	MCP16301T-E/CH
1	U2	ST	L78L05ACUTR	Farnell	1366573
2	U3, U4	Microchip	MCP2021A	microchipDirect	MCP2021A-330E/SN
1	U5	Microchip	PIC32MX775F256H	microchipDirect	PIC32MX775F256H
1	U6	Microchip	MCP2562	microchipDirect	MCP2562
1	Y1	VISHAY DALE	XT49M-8M	Farnell	1611765

Table V.1 Climate computer BOM

Subchapter 4 Layout

The climate computer layout structure is presented in *Figure V.7* and its 3D representation is presented in *Figure V.8*. The top connector is used for CAN connection (VBAT, CANH, CANL and GND), the right connector is used for the two LIN buses (VBAT, LIN1, LIN2 and GND). On the left side we have the external UART connector (top) and the programming connector for the microcontroller (bottom).

In the central part of the board we can find the microcontroller and its external oscillator (8 MHz crystal). Also, for debugging purposes, the board has 4 LEDs in the top-left side.

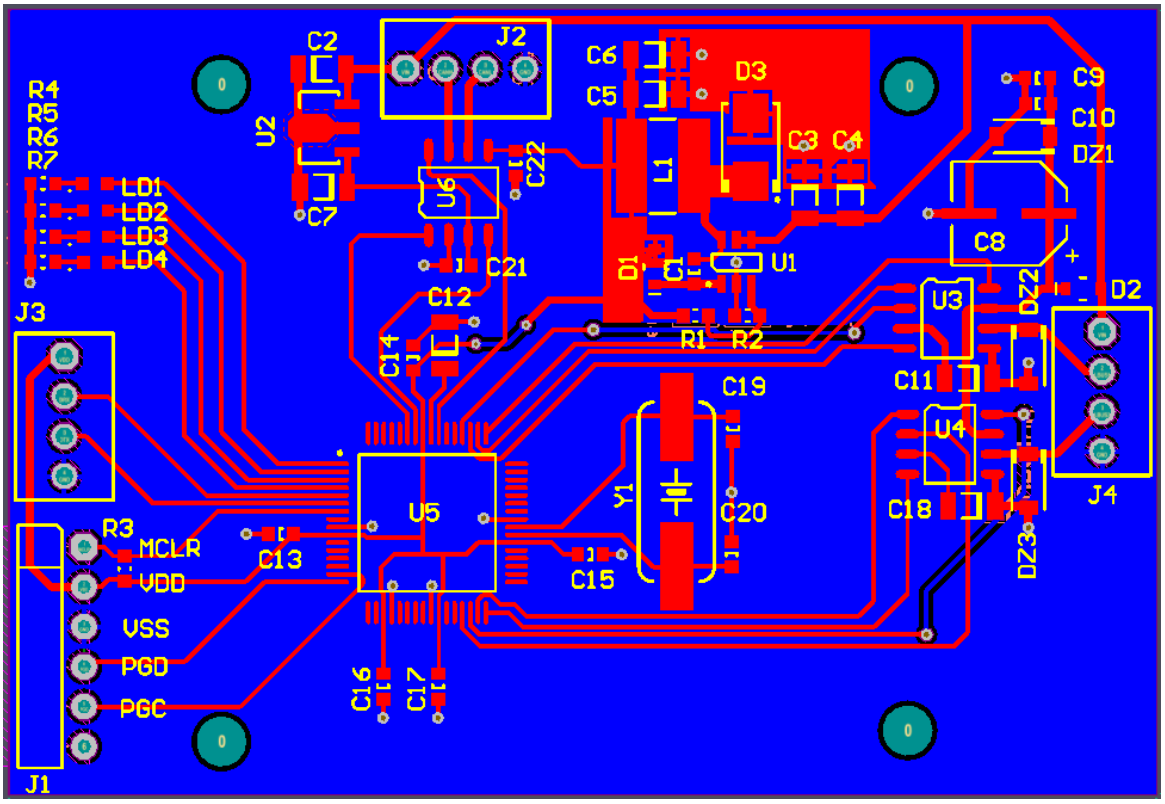

Figure V.7 Climate computer layout

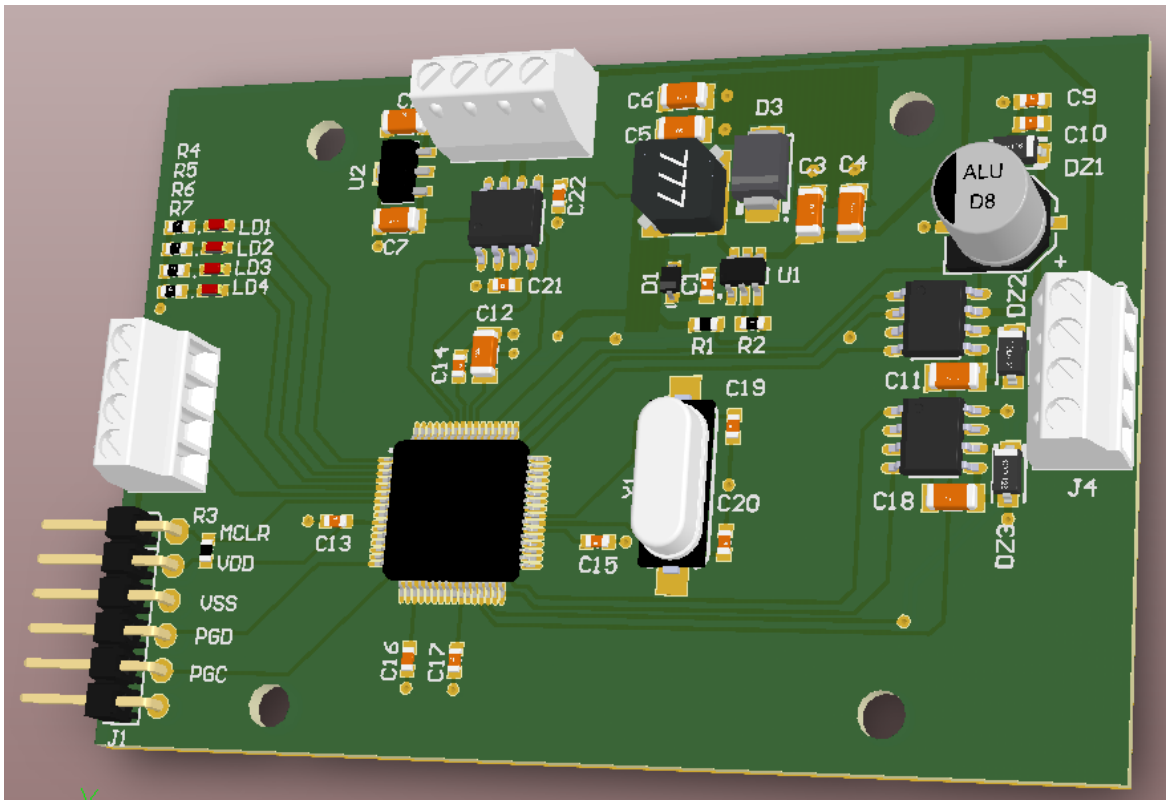

Figure V.8 Climate computer board - 3D view

Chapter VI. Conclusions and further improvement

In this paper a 4-zone climate control system was built from scratch, presenting the main actors and their role in the system. We have mentioned everything but the AC compressor's design, the back window defroster and the temperature sensors in detail (provided that the control dashboard is already integrated by the manufacturer).

For an electric AC compressor, the control hardware is 100% identical to the blower's hardware, except that it may require higher currents. The software, as well, would be unchanged if the compressor motor is a PMSM.

For the back window defroster the circuit is very simple: a circuit with LIN transceiver, a microcontroller for communication and for turning on and off a high current MOSFET transistor which opens or closes the circuit through the heating resistor on the window. In order to have better control over the heating system, a shunt measurement could be used to measure the current through the heating resistor, and the control could be done with using PWM.

The temperature sensors would be composed of a measuring sensor (which may have analog or serial type of output), a LIN transceiver and a microcontroller to read the temperature and forward it to the LIN bus. It is worth knowing that some manufacturers (seen in Mercedes-Benz manual (3)) also have very small and silent aspirators which blow interior air in the sensor. This is a very important detail which allows the whole control system to converge a lot faster: blowing air in the temperature sensor will indicate the real temperature a lot faster, which means the controller will have much accurate data for the measured value, which means a better response in time from the controller side.

As shortly presented above, detailed implementation (board implementation) of the three systems (AC compressor, back window defroster and temperature sensor board) seemed of little value-add to the paper.

Also there is worth knowing the following improvements (as could be seen on already existing systems) on the climate control system:

- some high-end cars have two blowers (SUVs mostly – the need to move and blow bigger volume of air);
- humidity sensors;
- solar panels to measure the solar radiation received by the car interior;
- LCD windows, which allows more or less solar radiation inside, reducing this way the total fuel consumption by not using the AC as much;
- Etc.

Further improvement of the currently discussed system, first of all, involves a consumption reduction mechanism (power consumption, not to be confused with fuel consumption). If considering only the trap doors and the blower, while they're off, we have about 21 LIN devices, which all have microcontrollers and transceivers. All these microcontrollers have an average consumption of 50 mA when fully functional. Considering 3.3V operation, the system consumes Pc watts of power, $Pc = 3.3V * 0.05\ A * 21\ devices$. Also considering the losses in the transceivers (some which transform the power with LDOs), the total power consumption is about 5W. All this consumption happens while the car is turned off. This gives around 150 hours of battery life, considering a 60Ah 12V battery. This is one unacceptable thing which must be improved. The electrical design present in the

paper allows this optimization to be done solely on software mode. The software should always put the microcontrollers and the transceivers in sleep mode when they're not used. This would give a total consumption, while car is off, of about 30mW, which now is feasible.

Also, one thing this paper does not treat is whether heating is present on electric cars. Since their first appearance on the commercial market, electric cars never used multi-zone climate control, due to the desire of maximizing the car autonomy. On electric cars, the motor (here motor should be referred as engine) efficiency may be high enough to provide less heat that can be distributed to the interior of the car. In this case, a heating resistor may be used instead of the mechanical valves. The circuit for the heating resistor would be the same as the one discussed above for the back window defroster, only much higher in terms of supported currents.

One more thing worth mentioning, on high end cars there can be an auxiliary heater, which gives the basis for interior preconditioning to temperature, based on a remote controller: the classic example would be turning on heat during the winter before the driver or passengers go inside the car, so the car would be already heated up. This is very simple to implement since the main controller unit of the climate system works on CAN. The remote controller receiver inside the car would then signal the main controller unit to start up and bring the temperature inside the car to a predefined one. The dashboard will also see the message and update the values.

Bibliography

1. *First Air-Conditioned Auto.* November 1933, Popular Science.
2. Automobile air conditioning. *Wikipedia.* [Online] http://en.wikipedia.org/wiki/Automobile_air_conditioning.
3. **Mercedes-Benz.** *Mercedes-Benz W220 Climate Control System Manual.* [Online] http://www.mercedestechstore.com/pdfs/507%20Systems%20I/507%20HO%20HVAC%20220%20%28ACB,%20IC%29%2010-30-02.pdf.
4. —. *Mercedes-Benz W210 Climate Control System Manual.* [Online] http://www.mercedestechstore.com/pdfs/W211_advisor/219%20HO%20HVAC%20%28TWK%29%208-30-02.pdf.
5. AUDI Q7 FAQ. *MyTurboDiesel.* [Online] http://www.myturbodiesel.com/1000q/q7/2010-2011-audi-q7-tdi-forum-faq.htm.
6. Local Interconnect Network. *Wikipedia.* [Online] http://en.wikipedia.org/wiki/Local_Interconnect_Network.
7. CAN bus. *Wikipedia.* [Online] http://en.wikipedia.org/wiki/CAN_bus.
8. **Torres, Daniel and Zambada, Jorge.** *AN1299 - Single-Shunt Three-Phase Current Reconstruction Algorithm for Sensorless FOC of a PMSM.* s.l. : Microchip Technology Inc., 2009.
9. **Jorge Zambada, Debraj Deb.** *AN1078 - Sensorless Field Oriented Control of a PMSM.* s.l. : Microchip Technology Inc.
10. Vector control (motor). *Wikipedia.* [Online] http://en.wikipedia.org/wiki/Vector_control_%28motor%29.
11. **Kedar Godbole, Texas Instruments.** Field oriented control reduces motor size, cost and power consumption in industrial applications. *EETimes.* [Online] http://eetimes.com/design/industrial-control/4013679/Field-oriented-control-reduces-motor-size-cost-and-power-consumption-in-industrial-applications?pageNumber=0.
12. Space vector modulation. *Wikipedia.* [Online] http://en.wikipedia.org/wiki/Space_vector_modulation.
13. **Reston Condit, Dr. Douglas W. Jones - University of Iowa.** *AN907 - Stepping motor fundamentals.* s.l. : Microchip Technology Inc.
14. *AN1307 - Stepper Motor Control with dsPIC® DSCs.* s.l. : Microchip Technology Inc.
15. Fuzzy Logic. *Wikipedia.* [Online] http://en.wikipedia.org/wiki/Fuzzy_logic.

Appendix A. Patents

1. Dual zone automatic climate control algorithm utilizing heat flux analysis
   US 20040164171 A1

2. Sunload sensor for automatic climate control systems
   US 5957375 A

3. HVAC control system for a multi-zoned vehicle
   US 6460356 B1

Appendix B. Copyright information